Int. J. Solids Structures Vol. 29, No. 4, pp. 437–463, 1992
Printed in Great Britain.

0020–7683/92 $5.00 + .00

SHAPE SENSITIVITY ANALYSIS AND OPTIMAL DESIGN OF DISKS AND PLATES WITH STRONG DISCONTINUITIES OF KINEMATIC FIELDS

K. DEMS
Łódź Technical University J26, ul. Zwirki 36, 90-924 Łódź, Poland

and

Z. MRÓZ
Institute of Fundamental Technological Research, Warsaw, Poland

(*Received* 19 *November* 1990; *in revised form* 5 *April* 1991)

Abstract—Disks, plates or beams subjected to loading and initial strains or displacements are assumed to be composed of portions interconnected by hinge or slip and dilatancy lines admitting discontinuities in displacements or slopes. The shape of such lines and their stiffness properties are subjected to variation. The sensitivity analysis is first discussed for an arbitrary functional of generalized stress, strain, displacement and boundary traction. The variation of complementary and potential energies is considered as a particular case of a general derivation for sensitivity. The optimal design problem is then considered and the relevant optimality conditions are derived. The general theory is illustrated by examples of sensitivity analysis and optimal design with respect to shape, position and stiffness of discontinuity lines for disks, plates and beams. Numerical aspects of sensitivity analysis are also discussed.

1. INTRODUCTION

The present work is concerned with disks and plates subjected to stretching and flexure. Small strain and displacement theory is used. However, the results can easily be extended to moderate or large deflection and strain theories. When mixed boundary conditions are imposed or an initial strain field is present, the stress level in the structure can be reduced by introducing kinematic discontinuity lines, that is slip lines or hinge lines. Along such lines the displacements or their gradients suffer discontinuities. The elastic energy stored along the discontinuity lines is a fraction of kinematic discontinuity, and the conjugate interface tractions are generated by the potential constitutive laws. Hinge line or slip line compliance is therefore an additional material parameter or function.

It is assumed that position, shape and/or compliance of the discontinuity line may vary, and the sensitivity analysis is performed with respect to these variations, considering an integral response functional. Next, the optimal design problem is considered, for which the optimal shape, position and compliance of the discontinuity line is sought in order to minimize the objective functional.

The present formulation constitutes an extension of a class of problems for which an optimal location, stiffness and prestress of elastic supports was determined for structures subjected to both loading and boundary displacements or initial distortions, cf. Mróz (1986, 1987), Garstecki and Mróz (1987). Optimal design of joints in elastic beams was considered by Garstecki (1988) where the relevant optimality criteria were derived and applied to some cases of beams and frames with the initial distortions imposed. A related work by Dems *et al.* (1989) is concerned with optimal design and sensitivity analysis of plates and disks with line stiffeners of unspecified shape, position and stiffness. The line stiffeners induced discontinuity in surface tractions with continuous displacement fields. In the present case the tractions are continuous along the kinematic discontinuity lines. Whereas the previous case involved an additional stiffening or strengthening of a structure by line actions, the geometric constraints are now relaxed, thus leading to more compliant designs. However, such designs are requisite when displacement or initial strain fields are imposed. In general there is a conflicting design situation: for applied loading, a structure should have sufficient stiffness and strength, for applied displacement it should be easily deformable. For mixed

type of loading there is a trade-off between displacement and stress levels, so both stress and displacement constraints should be considered. The examples of design for such cases were presented by Garstecki and Mróz (1987) and Garstecki (1988).

Though in general the design sensitivity analysis can be performed by using the direct or adjoint approaches, here, following Dems and Mróz (1984, 1985), only the adjoint variable method will be applied. This method requires only one additional solution of an adjoint boundary value problem for each specified functional independently of the number of design variables or parameters specifying properties and shape of the discontinuity line.

In Sections 2 and 3 the sensitivity analysis for disks and plates will be carried out and the optimality conditions will then be generated in Section 4. In Section 5 some aspects of numerical implementation of sensitivity analysis through the finite element method will be discussed. Several illustrative examples will be presented in Section 6.

2. SENSITIVITY ANALYSIS FOR DISKS WITH DISPLACEMENT DISCONTINUITY LINES

In this section, we shall consider a disk occupying the domain A with the boundary S (cf. Fig. 1a), which is subjected to stretching within its plane. Let us assume now that there exists within the disk domain A a line Γ, along which the displacement vector $\mathbf{u}$ can undergo some discontinuities while the tractions $\mathbf{N}$ transferred across the line are continuous. The generalized strains, stresses and body forces within the disk domain will be denoted by $\mathbf{q}$, $\mathbf{Q}$ and $\mathbf{f}$, respectively. Furthermore, it is assumed that the disk can be subjected to imposed fields of initial strains and stresses $\mathbf{q}^0$ and $\mathbf{Q}^0$ caused, for instance, by temperature fields or assemblage errors. The disk is loaded by the surface tractions $\tilde{\mathbf{N}}$ along boundary part S_T of its boundary S, while on the remaining boundary portion S_u the displacements $\tilde{\mathbf{u}}$ are prescribed, so that $S = S_T \cup S_u$.

The generalized nonlinear stress–strain relation within disk domain is generated by strain potential, such that

$$\mathbf{Q} = \frac{\partial U^A(\mathbf{q}, \mathbf{q}^0, \mathbf{Q}^0)}{\partial \mathbf{q}} = \mathbf{S}(\mathbf{q}, \mathbf{q}^0, \mathbf{Q}^0) \quad \text{within } A \tag{1}$$

where U^A denotes the specific strain energy per unit disk area. The incremental form of eqn (1) can be expressed as follows:

$$d\mathbf{Q} = \mathbf{D} \cdot d\mathbf{q} + \mathbf{Z} \cdot d\mathbf{q}^0 + \mathbf{L} \cdot d\mathbf{q}^0 \tag{2}$$

where

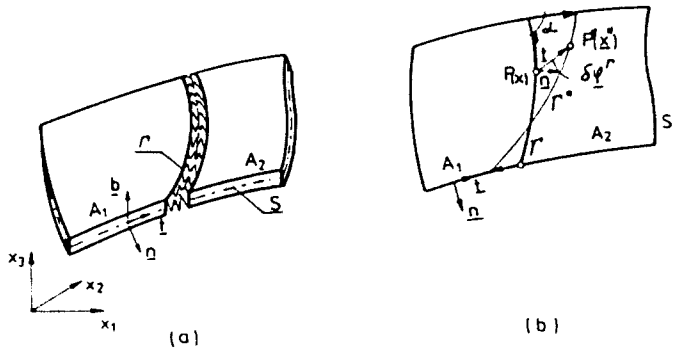

Fig. 1. Thin plate with discontinuity line (a) and its model (b).

$$\mathbf{D} = \frac{\partial^2 U^A}{\partial \mathbf{q}\,\partial \mathbf{q}} = \frac{\partial \mathbf{S}}{\partial \mathbf{q}}, \quad \mathbf{Z} = \frac{\partial \mathbf{S}}{\partial \mathbf{q}^i}, \quad \mathbf{L} = \frac{\partial \mathbf{S}}{\partial \mathbf{Q}^i} \tag{3}$$

and the dot between two symbols denotes the summation with respect to indices of lower order tensors. For a stable elastic material, $\mathbf{D}$ is a symmetric and positive definite tangent stiffness matrix, whereas $\mathbf{Z}$ and $\mathbf{L}$ represent the increments of elastic stresses due to increments of initial fields $\mathbf{q}^i$ and $\mathbf{Q}^i$.

Let us now denote by $\mathbf{v}$ the jump of displacement vector $\mathbf{u}$ along the line Γ, which will be called the discontinuity line (or slip and/or dilatancy line depending whether the tangential or normal displacement component suffers discontinuity). Thus, we can write

$$\mathbf{v}(\mathbf{x}) = [\![\mathbf{u}(\mathbf{x})]\!] = \mathbf{u}_2(\mathbf{x}) - \mathbf{u}_1(\mathbf{x}) \quad \mathbf{x} \in \Gamma \tag{4}$$

where $\mathbf{u}_1$ and $\mathbf{u}_2$ denote the disk displacements on both sides of line Γ. In what follows, we assume that the discontinuity vector $\mathbf{v}$ is related to continuous internal tractions $\mathbf{N}$ along Γ through the generalized nonlinear relation which can be generated by the potential U^Γ, such that

$$\mathbf{N} = \frac{\partial U^\Gamma(\mathbf{v}, \mathbf{c})}{\partial \mathbf{v}} = \mathbf{C}(\mathbf{v}, \mathbf{c}) \quad \text{along } \Gamma \tag{5}$$

where $\mathbf{c}$ denotes the set of design variables or parameters modifying the material properties of discontinuity line Γ. In order to simplify our analysis, we do not impose any restriction on the sign of the discontinuity vector $\mathbf{v}$ along Γ. The unilateral constraints are thus neglected in this analysis. The incremental form of eqn (5) can now be expressed as follows:

$$d\mathbf{N} = \mathbf{E} \cdot d\mathbf{v} + \mathbf{H} \cdot d\mathbf{c} \tag{6}$$

where

$$\mathbf{E} = \frac{\partial \mathbf{C}}{\partial \mathbf{v}}, \quad \mathbf{H} = \frac{\partial \mathbf{C}}{\partial \mathbf{c}} \tag{7}$$

denote the increment of internal tractions due to increment of discontinuity vector $\mathbf{v}$ and of design variables $\mathbf{c}$, respectively.

For such disk, the boundary-value problem can be solved for a specified geometry, loading and material properties of disk and discontinuity line and then the stress, strain and displacement distributions can be determined. Consider now a more complex problem when the material properties and shape of discontinuity line are not specified in advance. The major question can be posed as how the state fields or some global functionals are modified due to variations of material and geometrical properties of the discontinuity line. In analyzing this problem, we assume that besides the dependence of eqn (5) on a set of material design variables $\mathbf{c}$, the shape of line Γ is dependent on a set of shape design functions $\varphi_k(\mathbf{x})$, $k = 1, 2$, $\mathbf{x} \in \Gamma$ (cf. Fig. 1b). When the shape of Γ undergoes the shape variation $\delta\varphi(\Gamma)$, it is also assumed that the disk domain A may undergo the infinitesimal transformation $\delta\varphi(A)$, where $\partial\varphi$ is a differentiable vector field satisfying the conditions

$$\delta\varphi(A) = \delta\varphi(\Gamma) \quad \text{for } \mathbf{x} \in \Gamma, \quad \delta\varphi \cdot \mathbf{n} = 0 \quad \text{for } \mathbf{x} \in S. \tag{8}$$

Thus the external disk boundary does not undergo any normal shape transformation. On the other hand, when the discontinuity line penetrates the external boundary, the tangential shape transformation may occur. In this case, the additional constraint on the vector field $\delta\varphi$ at the end points of Γ is to be imposed, namely

$$\delta\varphi_s + \delta\varphi_n \cot\alpha = 0 \tag{9}$$

where $\delta\varphi_s$ and $\delta\varphi_n$ are the tangential and normal components of shape variation of Γ and α denotes the angle between Γ and S (cf. Fig. 1b).

Due to infinitesimal transformation of discontinuity line shape, the variations of orientation of the local coordinate system $\mathbf{n}, \mathbf{t}$ and of line length $d\Gamma$ and its curvature K occur, that is (cf. Dems and Mróz, 1984, 1987):

$$\begin{aligned}
&\hat{\delta}\mathbf{t} = \mathbf{n}(K\delta\varphi_s + \delta\varphi_{n,s}), \quad \hat{\delta}\mathbf{n} = -\mathbf{t}(K\delta\varphi_s + \delta\varphi_{n,s}) \\
&\delta(d\Gamma) = (\delta\varphi_{s,s} - K\delta\varphi_n), \quad \delta K = K_{,s}\delta\varphi_s + K^2\delta\varphi_n + \delta\varphi_{n,ss} \\
&\delta(dA) = \delta\varphi_{k,k}\, dA
\end{aligned} \tag{10}$$

where s denotes the line parameter, $\hat{\delta}$ is the total variation of any vector quantity and δ denotes the variation of any scalar quantity.

In performing the shape sensitivity analysis, following Dems and Mróz (1987, 1989) and Dems *et al.* (1989), besides the total variation $\hat{\delta}\mathbf{f}$ of any vector or tensor field $\mathbf{f}$, we introduce the local (i.e. for unperturbed domain) variation $\bar{\delta}\mathbf{f}$ of this field with respect to fixed Cartesian coordinate system (x_1, x_2), as well as the corotational variation $\delta\mathbf{f}$ with respect to local coordinate system $(\mathbf{n}, \mathbf{t})$ moving together with transformed discontinuity line Γ or external boundary S. The corotational variations do not take into account the rotation of coordinate system during the transformation process. If we denote the components of $\mathbf{f}$ with respect to fixed coordinate system by f_i, $i = 1, 2$, and with respect to local system by f_α, $\alpha = n, s$, then the relations between total, local and corotational variations of field $\mathbf{f}$ can be written as follows:

$$\begin{aligned}
&\hat{\delta} f_i = \bar{\delta} f_i + f_{i,k}\delta\varphi_k, \quad \hat{\delta} f_n = \delta f_n + f_s(K\delta\varphi_s + \delta\varphi_{n,s}), \\
&\hat{\delta} f_s = \delta f_s - f_n(K\delta\varphi_s + \delta\varphi_{n,s}).
\end{aligned} \tag{11}$$

Consider now any statically admissible stress field $\mathbf{Q}^s$ and kinematically compatible strain field $\mathbf{q}^k$. In view of equilibrium equations, strain displacement relations and eqns (10) and (11), the virtual work equation for simultaneous variations of kinematic fields and shape of discontinuity line can be written in the form

$$\begin{aligned}
&\int (\mathbf{Q}^s \cdot \bar{\delta}\mathbf{q}^k - \mathbf{f}^s \cdot \bar{\delta}\mathbf{u}^k)\, dA + \int N^s_{n\alpha}(\delta v^k_\alpha - v^k_{\alpha,\beta}\delta\varphi_\beta)\, d\Gamma - \int N^s_{n\alpha}(\delta u^k_\alpha - u^k_{\alpha,s}\delta\varphi_s)\, dS \\
&\qquad + \int [-e_{3\alpha\beta}(N^s_{n\alpha} v^k_\beta)_{,s}\delta\varphi_n + e_{3\alpha\beta}(N^s_{n\alpha} v^k_n \delta\varphi_n)_{,s}]\, d\Gamma \quad (\alpha, \beta = n, s)
\end{aligned} \tag{12}$$

where $N^s_{n\alpha}$ are the local components of surface tractions along line Γ and S, u^k_α and v^k_α are the local components of displacements along S and their jump along Γ and $e_{3\alpha\beta}$ denotes the permutation symbol. Equation (12) will be applied in deriving the sensitivity expressions.

2.1. *Sensitivity analysis for an arbitrary functional*

Let us now consider the functional

$$G = \int \Psi(\mathbf{Q}, \mathbf{q}, \mathbf{f}, \mathbf{u}, \mathbf{Q}^s, \mathbf{q}^s)\, dA + \int h(N_{n\alpha}, u_\alpha)\, dS + \int \Phi(N_{n\alpha}, v_\alpha, \mathbf{c})\, d\Gamma \tag{13}$$

where $N_{n\alpha}$, u_α and v_α denote the components of respective fields in local coordinate system $\mathbf{n}, \mathbf{t}$ along S and Γ. We assume furthermore that Ψ, h and Φ are continuous functions of their arguments, and that domains of integration A, S and Γ depend on the transformation

vector field $\varphi(\mathbf{x})$ associated with modification of shape of discontinuity line Γ. The variation $\delta\varphi(\mathbf{x})$ satisfies conditions (8) and (9).

The main purpose of this section is to determine the first variation of functional (13) associated with the variations of transformation field $\varphi(\mathbf{x})$ and of the set of parameters $\mathbf{c}$ along Γ, using the adjoint variable method. To start our analysis, let us introduce, besides the primary disk for which functional (13) is considered, the physically linear adjoint disk of the same geometry as the primary one. The adjoint disk with prescribed displacements, $\tilde{\mathbf{u}}^a$, on supported boundary part S_u, is loaded by surface tractions $\tilde{\mathbf{N}}^a$ on the remaining boundary portion S_T and body forces $\mathbf{f}^a$ within its domain A. Moreover, we assume that there exist the imposed fields of initial strains $\mathbf{q}^{ai}$ and stresses $\mathbf{Q}^{ai}$ within disk domain A, and initial jump of displacements $\mathbf{v}^{ai}$ and initial continuous tractions $\mathbf{N}^{ai}$ along discontinuity line Γ. The stress field $\mathbf{Q}^a$ within the adjoint disk satisfies the equilibrium and boundary conditions, and the strains $\mathbf{q}^a$ follow from displacement field $\mathbf{u}^a$ within A with the jump $\mathbf{v}^a$ along Γ. The generalized stress–strain relation for adjoint fields within A and the relation between the jump of displacements and continuous internal tractions along discontinuity line Γ are assumed in the form

$$\begin{aligned} \mathbf{Q}^a &= \mathbf{D}^T\cdot(\mathbf{q}^a-\mathbf{q}^{ai})-\mathbf{Q}^{ai} \quad \text{within } A \\ \mathbf{N}^a &= \mathbf{E}^T\cdot(\mathbf{v}^a-\mathbf{v}^{ai})-\mathbf{N}^{ai} \quad \text{along } \Gamma \end{aligned} \tag{14}$$

where the matrices $\mathbf{D}$ and $\mathbf{E}$ are specified by eqns (3) and (7). In view of virtual work equation for primary static fields and adjoint kinematic fields, the functional (13) can be rewritten in the following extended form:

$$G=\int\Psi\,dA+\int h\,dS+\int\Phi\,d\Gamma-\int(\mathbf{Q}\cdot\mathbf{q}^a-\mathbf{f}\cdot\mathbf{u}^a)\,dA-\int\mathbf{N}\cdot\mathbf{v}^a\,d\Gamma+\int\mathbf{N}\cdot\mathbf{u}^a\,dS \tag{15}$$

in which the sum of last three integrals on the right-hand side is equal to zero.

Consider now the first variation of functional (15). Following the analysis presented by Dems and Mróz (1989) and using eqns (10) and (11), the first variation of (15) can be presented as follows:

$$\begin{aligned} \delta G=&\int(\Psi_{,\mathbf{Q}}\cdot\bar{\delta}\mathbf{Q}+\Psi_{,\mathbf{q}}\cdot\bar{\delta}\mathbf{q}+\Psi_{,\mathbf{f}}\cdot\bar{\delta}\mathbf{f}+\Psi_{,\mathbf{u}}\cdot\bar{\delta}\mathbf{u}+\Psi_{,\mathbf{Q}^i}\cdot\bar{\delta}\mathbf{Q}^i \\ &+\Psi_{,\mathbf{q}^i}\cdot\bar{\delta}\mathbf{q}^i)\,dA-\int[\![\Psi]\!]\delta\varphi_n\,d\Gamma+\int[h_{,N_{nz}}(\delta N_{nz}-N_{nz,s}\delta\varphi_s) \\ &+h_{,u_z}(\delta u_z-u_{z,s}\delta\varphi_s)+(h\delta\varphi_s)_{,s}]\,dS+\int[\Phi_{,N_{nz}}(\delta N_{nz}-N_{nz,s}\delta\varphi_s) \\ &+\Phi_{,v_z}(\delta v_z-v_{z,s}\delta\varphi_s)+(\Phi\delta\varphi_s)_{,s}-\Phi K\delta\varphi_n]\,d\Gamma+\int\Phi_{,\mathbf{c}}\cdot(\bar{\delta}\mathbf{c}+\delta_n\mathbf{c})\,d\Gamma \\ &-\int(\bar{\delta}\mathbf{Q}\cdot\mathbf{q}^a+\mathbf{Q}\cdot\bar{\delta}\mathbf{q}^a-\bar{\delta}\mathbf{f}\cdot\mathbf{u}^a-\mathbf{f}\cdot\bar{\delta}\mathbf{u}^a)\,dA+\int([\![\mathbf{Q}\cdot\mathbf{q}^a]\!]-[\![\mathbf{f}\cdot\mathbf{u}^a]\!])\delta\varphi_n\,d\Gamma \\ &-\int[(\delta N_{nz}-N_{nz,s}\delta\varphi_s)v_z^a+N_{nz}(\delta v_z^a-v_{z,s}^a\delta\varphi_s)+(N_{nz}v_z^a\delta\varphi_s)_{,s} \\ &-N_{nz}v_z^aK\delta\varphi_n]\,d\Gamma+\int[(\delta N_{nz}-N_{nz,s}\delta\varphi_s)u_z^a+N_{nz}(\delta u_z^a-u_{z,s}^a\delta\varphi_s) \\ &+(N_{nz}u_z^a\delta\varphi_s)_{,s}]\,dS \end{aligned} \tag{16}$$

where $[\![\cdot]\!]$ denotes the jump of enclosed quantity along Γ, calculated as its difference on the right and left side of Γ, $\bar{\delta}\mathbf{c}$ is the local variation of parameters $\mathbf{c}$ for unperturbed shape of discontinuity line and $\delta_n\mathbf{c}$ denotes the variation of $\mathbf{c}$ due to normal shape variation of Γ.

Using now the incremental forms of constitutive equations (2) and (6) of primary disk and constitutive laws (14) of adjoint disk, one can write

$$\bar{\delta}\mathbf{Q}\cdot\mathbf{q}^{\mathrm{a}} = \mathbf{Q}^{\mathrm{a}}\cdot\bar{\delta}\mathbf{q} + \mathbf{Q}^{\mathrm{at}}\cdot\bar{\delta}\mathbf{q} + \mathbf{q}^{\mathrm{at}}\cdot\bar{\delta}\mathbf{Q} = (\mathbf{q}^{\mathrm{a}} - \mathbf{q}^{\mathrm{at}})\cdot(\mathbf{L}\cdot\bar{\delta}\mathbf{Q}^{\mathrm{t}} + \mathbf{Z}\cdot\bar{\delta}\mathbf{q}^{\mathrm{t}}) \quad \text{within } A$$

$$\delta N_{n\alpha}v_\alpha^{\mathrm{a}} = N_{n\alpha}^{\mathrm{a}}\delta v_\alpha + N_{n\alpha}^{\mathrm{at}}\delta v_\alpha + v_\alpha^{\mathrm{at}}\delta N_{n\alpha} + (v_\alpha^{\mathrm{a}} - v_\alpha^{\mathrm{at}})H_{\alpha l}(\bar{\delta}c_l + \delta_n c_l)$$
$$+ [N_{n\alpha,s}(v_\alpha^{\mathrm{a}} - v_\alpha^{\mathrm{at}}) - (N_{n\alpha}^{\mathrm{a}} + N_{n\alpha}^{\mathrm{at}})v_{\alpha,s}]\delta\varphi_s \quad \text{along } \Gamma. \tag{17}$$

Now, we can substitute relations (17) into eqn (16) and apply to it the virtual work eqn (12) twice. We first write eqn (12) for primary static fields $\mathbf{Q}$, $\mathbf{f}$, $\mathbf{N}$ and adjoint kinematic fields $\mathbf{q}^{\mathrm{a}}$, $\mathbf{u}^{\mathrm{a}}$, $\mathbf{v}^{\mathrm{a}}$, and next use it for primary kinematic fields $\mathbf{q}$, $\mathbf{u}$, $\mathbf{v}$ and adjoint static fields $\mathbf{Q}^{\mathrm{a}}$, $\mathbf{f}^{\mathrm{a}}$, $\mathbf{N}^{\mathrm{a}}$. After some transformation, the first variation (16) of an arbitrary functional G takes the form

$$\delta G = \int_A \{(u_i^{\mathrm{a}} + \Psi_{,f_i})\bar{\delta}f_i + [\Psi_{,Q_{ij}} - (q_{kl}^{\mathrm{a}} - q_{kl}^{\mathrm{at}})L_{ij,kl}]\bar{\delta}Q_{ij}$$
$$+ [\Psi_{,q_{ij}} - (q_{kl}^{\mathrm{a}} - q_{kl}^{\mathrm{at}})Z_{ij,kl}]\bar{\delta}q_{ij}^{\mathrm{t}}\}\,\mathrm{d}A + \int_{S_T}(h_{,N_{n\alpha}} + u_\alpha^{\mathrm{a}})(\delta N_{n\alpha} - N_{n\alpha,s}\delta\varphi_s)\,\mathrm{d}S_T$$
$$+ \int_{S_u}(h_{,u_\alpha} - N_{n\alpha}^{\mathrm{a}})(\delta u_\alpha - u_{\alpha,s}\delta\varphi_s)\,\mathrm{d}S_u + \int_\Gamma [(h + N_{n\alpha}u_\alpha^{\mathrm{a}})\delta\varphi_s]_{,s}\,\mathrm{d}S$$
$$+ \int_\Gamma \{[-[\![\Psi]\!] - \Phi K - [\![f_\alpha u_\alpha^{\mathrm{a}}]\!] + [\![Q_{\alpha\beta}q_{\alpha\beta}^{\mathrm{a}}]\!] + N_{n\alpha}v_\alpha^{\mathrm{a}}K - N_{n\alpha}v_{\alpha,n}^{\mathrm{a}}$$
$$- N_{n\alpha}^{\mathrm{a}}v_{\alpha,n} + e_{3\alpha\beta}(N_{n\alpha}v_\beta^{\mathrm{a}} + N_{n\alpha}^{\mathrm{a}}v_\beta)_{,s}]\delta\varphi_n + [(\Phi - N_{n\alpha}v_\alpha^{\mathrm{a}})\delta\varphi_s$$
$$- e_{3\alpha\beta}(N_{n\alpha}v_\beta^{\mathrm{a}} + N_{n\alpha}^{\mathrm{a}}v_\beta)\delta\varphi_n]_{,s}\}\,\mathrm{d}\Gamma + \int_\Gamma [\Phi_{,c_l} - (v_\alpha^{\mathrm{a}} - v_\alpha^{\mathrm{at}})H_{\alpha l}]$$
$$\times(\bar{\delta}c_l + \delta_n c_l)\,\mathrm{d}\Gamma + \int_A \{(\Psi_{,Q_{ij}} - q_{ij}^{\mathrm{at}})\bar{\delta}Q_{ij} + (\Psi_{,q_{ij}} - Q_{ij}^{\mathrm{at}})\bar{\delta}q_{ij}$$
$$+ (\psi_{,u_i} - f_i^{\mathrm{a}})\bar{\delta}u_i\}\,\mathrm{d}A + \int_{S_u}(h_{,N_{n\alpha}} + u_\alpha^{\mathrm{a}})(\delta N_{n\alpha} - N_{n\alpha,s}\delta\varphi_s)\,\mathrm{d}S_u$$
$$+ \int_{S_T}(h_{,u_\alpha} - N_{n\alpha}^{\mathrm{a}})(\delta u_\alpha - u_{\alpha,s}\delta\varphi_s)\,\mathrm{d}S_T + \int_\Gamma [(\Phi_{,N_{n\alpha}} - v_\alpha^{\mathrm{at}})(\delta N_{n\alpha} - N_{n\alpha,s}\delta\varphi_s)$$
$$+ (\Phi_{,v_\alpha} - N_{n\alpha}^{\mathrm{at}})(\delta v_\alpha - v_{\alpha,s}\delta\varphi_s)]\,\mathrm{d}\Gamma. \tag{18}$$

The last four integrals on the right-hand side of eqn (18), depending on local state field variations of the primary disk within its domain A and on corotational variations of state fields along boundary S and discontinuity line Γ, vanish when the imposed initial fields and boundary conditions of adjoint disk are assumed in the form

$$q_{ij}^{\mathrm{at}} = \Psi_{,Q_{ij}}, \quad Q_{ij}^{\mathrm{at}} = \Psi_{,q_{ij}}, \quad f_i^{\mathrm{a}} = \Psi_{,u_i} \quad \text{within } A$$
$$\tilde{u}_\alpha^{\mathrm{a}} = -h_{,N_{n\alpha}} \quad \text{on } S_u, \quad \tilde{N}_{n\alpha}^{\mathrm{a}} = h_{,u_\alpha} \quad \text{on } S_T$$
$$v_\alpha^{\mathrm{at}} = \Phi_{,N_{n\alpha}}, \quad N_{n\alpha}^{\mathrm{at}} = \Phi_{,v_\alpha} \quad \text{along } \Gamma. \tag{19}$$

Making use of conditions (19) and integrating some terms of eqn (18) along S and Γ, the first variation of G is finally expressed as follows

$$\delta G = \int \{(u_i^a + \Psi_{,f_i})\bar{\delta} f_i + [\Psi_{,Q^i_{ij}} - (q^a_{kl} - q^{ai}_{kl})L_{ijkl}]\bar{\delta} Q^i_{ij}$$

$$+ [\Psi_{,q^i_{ij}} - (q^a_{kl} - q^{ai}_{kl})Z_{ijkl}]\bar{\delta} q^i_{ij}\} \, dA + \int (h_{,N_{n\alpha}} + u^a_\alpha)(\delta N_{n\alpha} - N_{n\alpha,s}\delta\varphi_s) \, dS_T$$

$$+ \int (h_{,u_\alpha} - N^a_{n\alpha})(\delta u_\alpha - u_{\alpha,s}\delta\varphi_s) \, dS_u - \sum_k [\![(h + N_{n\alpha}u^a_\alpha)\delta\varphi_s]\!]|_{P^S_k}$$

$$+ \int [-[\![\Psi]\!] - \Phi K - [\![f_\alpha u^a_\alpha]\!] + [\![Q_{\alpha\beta}q^a_{\alpha\beta}]\!] + N_{n\alpha}v^a_\alpha K - N_{n\alpha}v^a_{\alpha,n}$$

$$- N^a_{n\alpha}v_{\alpha,n} + e_{3\alpha\beta}(N_{n\alpha}v^a_\beta + N^a_{n\alpha}v_\beta)_{,s}]\delta\varphi_n \, d\Gamma - \sum_k [\![(\Phi - N_{n\alpha}v^a_\alpha)\delta\varphi_s$$

$$- e_{3\alpha\beta}(N_{n\alpha}v^a_\beta + N^a_{n\alpha}v_\beta)\delta\varphi_n]\!]|_{P^\Gamma_k} + \int [\Phi_{,c_l} - (v^a_\alpha - v^{ai}_\alpha)H_{\alpha l}]$$

$$\times (\bar{\delta} c_l + \delta_n c_l) \, d\Gamma. \tag{20}$$

Thus, the first variation of G is expressed explicitly in terms of shape and material variations of discontinuity line, and depends on solutions of boundary value problems of primary and adjoint disks. The first three integrals on the right-hand side of eqn (20) express the share of δG caused by influence of shape variation of the discontinuity line on distribution of initial strains and stresses within disk domain and boundary displacements and tractions along parts S_u and S_T of its external boundary, respectively. The fourth and fifth integrals express explicitly the contribution in δG due to normal shape variation of Γ and variation of its material properties. Finally, the two remaining terms are the contributions in δG when the same singular points P^S_k and P^Γ_k occur along external boundary S or discontinuity line Γ. In these singular points either the enclosed quantities suffer some discontinuities or the lines S and Γ are not smooth.

2.2. *Sensitivity analysis for complementary and potential energies*

Consider now a particular case when the functional G coincides with the complementary or potential energies of a disk and particularize its first variation associated with shape and material variations of discontinuity line Γ. Such functionals occur in problems of global compliance or stiffness design. To simplify the sensitivity expressions let us assume that there are no singular points along S and Γ, and consider first the complementary energy of a disk that equals

$$\Pi_Q = \int W^A(\mathbf{Q}, \mathbf{Q}^i, \mathbf{q}^i) \, dA - \int \mathbf{N} \cdot \tilde{\mathbf{u}} \, dS_u + \int W^\Gamma(\mathbf{N}, \mathbf{c}) \, d\Gamma \tag{21}$$

where W^A denotes the specific stress energy per unit area of a disk and W^Γ is the elastic stress energy per unit length of discontinuity line. Comparing (21) with (13), we easily observe that

$$\Psi = W^A \quad \text{within } A, \quad h = \begin{cases} -\mathbf{N} \cdot \tilde{\mathbf{u}} & \text{on } S_u \\ 0 & \text{on } S_T \end{cases}, \quad \Phi = W^\Gamma \quad \text{along } \Gamma, \tag{22}$$

and then, according to (19), the adjoint disk has to satisfy the following boundary conditions:

$$\tilde{\mathbf{u}}^a = \tilde{\mathbf{u}} \quad \text{on } S_u, \quad \tilde{\mathbf{N}}^a = 0 \quad \text{on } S_T, \tag{23}$$

while the imposed initial fields are

$$\mathbf{q}^{a0} = W^A_{\mathbf{Q}} = \mathbf{q}, \quad \mathbf{Q}^{a0} = 0, \quad \mathbf{f}^a = 0 \quad \text{within } A$$
$$\mathbf{v}^{a0} = W^\Gamma_{\mathbf{N}} = \mathbf{v}, \quad \mathbf{N}^{a0} = 0 \quad \text{along } \Gamma. \tag{24}$$

Thus, the state fields within the adjoint disk are expressed in terms of solutions of primary disk, and they take the form

$$\mathbf{u}^a = \mathbf{u}, \quad \mathbf{q}^a = \mathbf{q}, \quad \mathbf{Q}^a = 0 \quad \text{within } A$$
$$\mathbf{v}^a = \mathbf{v}, \quad \mathbf{N}^a = 0 \quad \text{along } \Gamma. \tag{25}$$

In view of (22)–(25), eqn (20), expressing now the first variation of Π_Q, is simplified as follows

$$\delta\Pi_Q = \int (u_i \bar{\delta} f_i + W^A_{,Q'_{ij}} \bar{\delta} Q'_{ij} + W^A_{,q'_{ij}} \bar{\delta} q'_{ij})\, \mathrm{d}A + \int u_\alpha (\delta N_{n\alpha} - N_{n\alpha,s}\delta\varphi_s)\, \mathrm{d}S_T$$
$$- \int N_{n\alpha}(\delta u_\alpha - u_{\alpha,s}\delta\varphi_s)\, \mathrm{d}S_u + \int [-[\![W^A]\!] + [\![Q_{\alpha\beta}q_{\alpha\beta}]\!] - [\![f_\alpha u_\alpha]\!] + (N_{n\alpha}v_\alpha - W^\Gamma)K$$
$$- N_{n\alpha}v_{\alpha,n} + e_{3\alpha\beta}(N_{n\alpha}v_\beta)_{,s}]\delta\varphi_n\, \mathrm{d}\Gamma + \int W^\Gamma_{,c_l}(\bar{\delta}c_l + \delta_n c_l)\, \mathrm{d}\Gamma. \tag{26}$$

Assume now that the functional G coincides with the total potential energy of a disk and is expressed as

$$\Pi_u = \int [U^A(\mathbf{q}, \mathbf{Q}', \mathbf{q}') - \mathbf{f}\cdot\mathbf{u}]\, \mathrm{d}A - \int \tilde{\mathbf{N}}\cdot\mathbf{u}\, \mathrm{d}S_T + \int U^\Gamma(\mathbf{v}, \mathbf{c})\, \mathrm{d}\Gamma \tag{27}$$

where U^A and U^Γ denote the specific energies per unit area and length, respectively. Comparing (27) with (13), we have

$$\Psi = U^A - \mathbf{f}\cdot\mathbf{u} \quad \text{within } A, \quad h = \begin{cases} 0 & \text{on } S_u \\ -\tilde{\mathbf{N}}\cdot\mathbf{u} & \text{on } S_T \end{cases}, \quad \Phi = U^\Gamma \quad \text{along } \Gamma, \tag{28}$$

and then, the adjoint disk is subjected to the following boundary conditions and imposed initial fields

$$\tilde{\mathbf{u}}^a = 0 \quad \text{on } S_u, \quad \tilde{\mathbf{N}}^a = -\tilde{\mathbf{N}} \quad \text{on } S_T$$
$$\mathbf{q}^{a0} = 0, \quad \mathbf{Q}^{a0} = U^A_{\mathbf{q}} = \mathbf{Q}, \quad \mathbf{f}^a = U^A_{\mathbf{u}} = -\mathbf{f} \quad \text{within } A$$
$$\mathbf{v}^{a0} = 0, \quad \mathbf{N}^{a0} = U^\Gamma_{\mathbf{v}} = \mathbf{N} \quad \text{along } \Gamma. \tag{29}$$

The solutions of the adjoint disk are expressed in terms of primary state fields, namely

$$\mathbf{u}^a = 0, \quad \mathbf{q}^a = 0, \quad \mathbf{Q}^a = -\mathbf{Q} \quad \text{within } A$$
$$\mathbf{v}^a = 0, \quad \mathbf{N}^a = -\mathbf{N} \quad \text{along } \Gamma, \tag{30}$$

and eqn (20), expressing now the variation of Π_u, takes the form

$$\delta\Pi_n = \int (-u_i\bar{\delta}f_i + U^A_{,Q^i_{ij}}\bar{\delta}Q^i_{ij} + U^A_{,q^i_{ij}}\bar{\delta}q^i_{ij})\,\mathrm{d}A - \int u_\alpha(\delta N_{n\alpha} - N_{n\alpha,s}\delta\varphi_s)\,\mathrm{d}S_T$$

$$+ \int N_{n\alpha}(\delta u_\alpha - u_{\alpha,s}\delta\varphi_s)\,\mathrm{d}S_u + \int [-[\![U^A]\!] - U^\Gamma)K + N_{n\alpha}v_{\alpha,s}$$

$$- e_{3\alpha\beta}(N_{n\alpha}v_\beta)_{,s}]\delta\varphi_n\,\mathrm{d}\Gamma + \int U^\Gamma_{,c_l}(\bar{\delta}c_l + \delta_n c_l)\,\mathrm{d}\Gamma. \quad (31)$$

It is easy to verify that $\delta\Pi_Q = -\delta\Pi_u$ since $W^A + U^A = \mathbf{Q}\cdot\mathbf{q}$ and $W^\Gamma + U^\Gamma = \mathbf{N}\cdot\mathbf{v}$.

3. SENSITIVITY ANALYSIS FOR PLATE WITH KINEMATIC DISCONTINUITY LINE

Let us discuss in this Section the case of bending of a plate and derive the sensitivity expression for an arbitrary functional with respect to change of shape and material properties of kinematic discontinuity line within its domain.

The geometry of a plate is shown in Fig. 1. Denote by $\mathbf{M} = [M_{ij}] = [M_{\alpha\beta}]$ and $\boldsymbol{\kappa} = [\kappa_{ij}] = [\kappa_{\alpha\beta}]$ the generalized stress and strain tensors within plate domain, where, as in Section 2, the subscripts i, j denote the components of a proper tensor with respect to a fixed Cartesian coordinate system, and the subscripts α, β denote its components with respect to local system $\mathbf{n}, \mathbf{t}$. The generalized displacements and surface tractions are denoted by $\mathbf{w}$ and $\mathbf{R}$, where

$$\mathbf{w} = \{w_\zeta\} = \begin{Bmatrix} w \\ -w_{,n} \end{Bmatrix}, \quad \mathbf{R} = \{R_\zeta\} = \begin{Bmatrix} Q \\ M_{nn} \end{Bmatrix} \quad (32)$$

and Q, M_{nn} are generalized shear force and bending moment, respectively. The plate is subjected to a transverse load p, whereas the generalized tractions $\tilde{\mathbf{R}}$ are specified on external boundary part S_R and the generalized boundary displacements $\tilde{\mathbf{w}}$ are specified on the remaining part S_w. Moreover, the plate can be subjected to the imposed fields of initial strains $\boldsymbol{\kappa}^i$ and stresses $\mathbf{M}^i$. The generalized stress–strain relation within the plate domain is assumed in a form similar to (1), namely

$$\mathbf{M} = \frac{\partial U^A(\boldsymbol{\kappa}, \boldsymbol{\kappa}^i, \mathbf{M}^i)}{\partial \boldsymbol{\kappa}} = \mathbf{S}(\boldsymbol{\kappa}, \boldsymbol{\kappa}^i, \mathbf{M}^i) \quad (33)$$

where now U^A denotes the flexural specific strain energy.

As in Section 2, let us assume that the generalized displacements $\mathbf{w}$ along discontinuity line Γ within the plate domain can suffer some jump in deflection w and/or its normal derivative $-w_{,n}$, which will be denoted by $\mathbf{v}(\mathbf{x}) = \mathbf{w}_2(\mathbf{x}) - \mathbf{w}_1(\mathbf{x})$, $\mathbf{x} \in \Gamma$. The surface tractions $\mathbf{R}$ along Γ are still continuous and they are related to the kinematic discontinuity vector $\mathbf{v}$ by the relation similar to (5), namely

$$\mathbf{R} = \frac{\partial U^\Gamma(\mathbf{v}\cdot\mathbf{c})}{\partial \mathbf{v}} = \mathbf{C}(\mathbf{v}, \mathbf{c}). \quad (34)$$

Assuming now that the discontinuity line Γ can undergo the shape variation satisfying conditions (8) and (9), the virtual equation for simultaneous variations of kinematic fields and shape of Γ, in view of eqns (10) and (11), can be written in the form

$$\int (\mathbf{M}^s \cdot \bar{\delta}\boldsymbol{\kappa}^k - p^s \cdot \bar{\delta} w^k)\, dA + \int R_\xi^s (\delta v_\xi^k - v_{\xi,s}^k \delta\varphi_s)\, d\Gamma - \int R_\xi^s (\delta w_\xi^k - w_{\xi,s}^k \delta\varphi_s)\, dS$$

$$= \int [M_{ns}^s (\delta v^k - v_{,s}^k \delta\varphi_t) + (M_{nn}^s v_{,s}^k - M_{ns}^s v_{,n}^k)\delta\varphi_n]_{,s}\, d\Gamma - \int [M_{ns}^s (\delta w^k - w_{,s}^k \delta\varphi_t)]_{,s}\, dS. \quad (35)$$

where the statically admissible stress field $\mathbf{M}^s$ satisfies the equilibrium and boundary conditions and $\boldsymbol{\kappa}^k$ is kinematically compatible curvature field. Equation (35) will be used in the next section for determining the sensitivity expression.

As in Section 2, besides the primary plate, let us introduce an adjoint plate of the same geometry as the primary one, with imposed fields $\mathbf{M}^{a_1}$, $\boldsymbol{\kappa}^{a_1}$ of initial stresses and strains within plate domain A and initial jump of displacements $\mathbf{v}^{a_1}$ and initial continuous tractions $\mathbf{R}^{a_1}$ along discontinuity line Γ. The adjoint plate is subjected to the lateral pressure p^a within A and surface tractions $\tilde{\mathbf{R}}^a$ along S_R with prescribed displacements $\tilde{\mathbf{w}}^a$ along S_w. The particular form of loading and supporting conditions as well as initial fields depends on the functional to be considered and will be specified later on. The constitutitve laws for the adjoint plate are assumed in the form similar to (14), namely

$$\mathbf{M}^a = \mathbf{D}^T \cdot (\boldsymbol{\kappa}^a - \boldsymbol{\kappa}^{a_1}) - \mathbf{M}^{a_1} \quad \text{within } A$$

$$\mathbf{R}^a = \mathbf{E}^T \cdot (\mathbf{v}^a - \mathbf{v}^{a_1}) - \mathbf{R}^{a_1} \quad \text{along } \Gamma \quad (36)$$

where now $\mathbf{D} = \partial \mathbf{S}/\partial \boldsymbol{\kappa}$ and $\mathbf{E} = \partial \mathbf{C}/\partial \mathbf{v}$ following on from eqns (33) and (34), and can be regarded as the tangent stiffness matrices at the solution point. The stress field $\mathbf{M}^a$ satisfies the equilibrium and boundary conditions, whereas the adjoint total strains $\mathbf{q}^a$ follow from adjoint displacement field $\mathbf{w}^a$.

3.1. *Sensitivity analysis for an arbitrary functional*

As in Section 2, consider now the functional

$$G = \int \Psi(\mathbf{M}, \boldsymbol{\kappa}, p, w, \mathbf{M}^1, \boldsymbol{\kappa}^1)\, dA + \int h(R_\xi, w_\xi)\, dS + \int \Phi(R_\xi, v_\xi, \mathbf{c})\, d\Gamma \quad (37)$$

and derive its first variation with respect to variations of shape and material properties of discontinuity line Γ. The extended form of functional G, which constitutes the base for our foregoing analysis, in view of the reciprocal theorem, can be written as follows:

$$G = \int \psi\, dA + \int h\, dS + \int \Phi\, d\Gamma - \int (\mathbf{M} \cdot \boldsymbol{\kappa}^a - p w^a)\, dA$$

$$- \int [\mathbf{R} \cdot \mathbf{v}^a - (M_{ns} v^a)_{,s}]\, d\Gamma + \int \mathbf{R} \cdot \mathbf{w}^a - (M_{ns} w^a)_{,s}]\, dS. \quad (38)$$

It is obvious that the sum of the three last integrals on the right-hand side of eqn (38) is equal to zero, and so expressions (37) and (38) are identical.

Following the analysis of Dems and Mróz (1989) and using eqns (10) and (11), the first variation of (38) can be written in the form

$$\bar{\delta}G = \int (\Psi_{,\mathbf{M}} \cdot \bar{\delta}\mathbf{M} + \Psi_{,\kappa} \cdot \bar{\delta}\boldsymbol{\kappa} + \Psi_{,p}\bar{\delta}p + \Psi_{,w}\bar{\delta}w + \Psi_{,\mathbf{M}^{\mathrm{i}}} \cdot \bar{\delta}\mathbf{M}^{\mathrm{i}} + \Psi_{,\kappa^{\mathrm{i}}} \cdot \bar{\delta}\boldsymbol{\kappa}^{\mathrm{i}})\,\mathrm{d}A$$

$$- \int [\![\Psi]\!]\delta\varphi_n\,\mathrm{d}\Gamma + \int [h_{,R_\xi}(\delta R_\xi - R_{\xi,s}\delta\varphi_s) + h_{,w_\xi}(\delta w_\xi - w_{\xi,s}\delta\varphi_s)$$

$$+ (h\delta\varphi_s)_{,s}]\,\mathrm{d}S + \int [\Phi_{,R_\xi}(\delta R_\xi - R_{\xi,s}\delta\varphi_s) + \Phi_{,v_\xi}(\delta v_\xi - v_{\xi,s}\delta\varphi_s) + (\Phi\delta\varphi_s)_{,s}$$

$$- \Phi K\delta\varphi_n]\,\mathrm{d}\Gamma + \int \Phi_{,\mathbf{c}} \cdot (\bar{\delta}\mathbf{c} + \delta_n\mathbf{c})\,\mathrm{d}\Gamma - \int (\mathbf{M} \cdot \bar{\delta}\boldsymbol{\kappa}^{\mathrm{a}} - p\delta w^{\mathrm{a}})\,\mathrm{d}A$$

$$- \int R_\xi(\delta v_\xi^{\mathrm{a}} - v_{\xi,s}^{\mathrm{a}}\delta\varphi_s)\,\mathrm{d}\Gamma + \int R_\xi(\delta w_\xi^{\mathrm{a}} - w_{\xi,s}^{\mathrm{a}}\delta\varphi_s)\,\mathrm{d}S - \int (\bar{\delta}\mathbf{M} \cdot \boldsymbol{\kappa}^{\mathrm{a}} - \bar{\delta}pw^{\mathrm{a}})\,\mathrm{d}A$$

$$- \int (\delta R_\xi - R_{\xi,s}\delta\varphi_s)v_\xi^{\mathrm{a}}\,\mathrm{d}\Gamma + \int (\delta R_\xi - R_{\xi,s}\delta\varphi_s)w_\xi^{\mathrm{a}}\,\mathrm{d}S + \int ([\![\mathbf{M} \cdot \boldsymbol{\kappa}^{\mathrm{a}}]\!] - [\![pw^{\mathrm{a}}]\!])\delta\varphi_n\,\mathrm{d}\Gamma$$

$$- \int (R_\xi v_\xi^{\mathrm{a}}\delta\varphi_s)_{,s}\,\mathrm{d}\Gamma + \int (R_\xi w_\xi^{\mathrm{a}}\delta\varphi_s)_{,s}\,\mathrm{d}S + \int R_\xi v_\xi^{\mathrm{a}} K\delta\varphi_n\,\mathrm{d}\Gamma$$

$$+ \int [\delta(M_{ns}v^{\mathrm{a}})]_{,s}\,\mathrm{d}\Gamma - \int [\delta(M_{ns}w^{\mathrm{a}})]_{,s}\,\mathrm{d}S. \tag{39}$$

Using now the incremental form of constitutive eqns (33) and (34) of a primary plate, and applying eqns (36), the following identity can be written:

$$\int (\bar{\delta}M^{\mathrm{a}} \cdot \boldsymbol{\kappa}^{\mathrm{a}} - \bar{\delta}pw^{\mathrm{a}})\,\mathrm{d}A + \int \delta R_\xi - R_{\xi,s}\delta\varphi_s)v_\xi^{\mathrm{a}}\,\mathrm{d}\Gamma = \int (\mathbf{M}^{\mathrm{a}} \cdot \bar{\delta}\boldsymbol{\kappa} - p^{\mathrm{a}}\bar{\delta}w)\,\mathrm{d}A$$

$$+ \int [p^{\mathrm{a}}\bar{\delta}w - \bar{\delta}pw^{\mathrm{a}} + \mathbf{M}^{\mathrm{ai}} \cdot \bar{\delta}\boldsymbol{\kappa} + \boldsymbol{\kappa}^{\mathrm{ai}} \cdot \bar{\delta}\mathbf{M} + (\boldsymbol{\kappa}^{\mathrm{a}} - \boldsymbol{\kappa}^{\mathrm{ai}}) \cdot (\mathbf{L} \cdot \bar{\delta}\mathbf{M}^{\mathrm{i}} + \mathbf{Z} \cdot \bar{\delta}\boldsymbol{\kappa}^{\mathrm{i}})]\,\mathrm{d}A$$

$$+ \int [R_\xi^{\mathrm{a}}(\delta v_\xi - v_{\xi,s}\delta\varphi_s) + R_\xi^{\mathrm{ai}}(\delta v_\xi - v_{\xi,s}\delta\varphi_s) + v_\xi^{\mathrm{ai}}(\delta R_\xi - R_{\xi,s}\delta\varphi_s)$$

$$+ (v_\xi^{\mathrm{a}} - v_\xi^{\mathrm{ai}})H_{\xi j}(\bar{\delta}c_j + \delta_n c_j)]\,\mathrm{d}\Gamma \tag{40}$$

where

$$\mathbf{L} = \frac{\partial \mathbf{S}}{\partial \mathbf{M}^{\mathrm{i}}}, \quad \mathbf{Z} = \frac{\partial \mathbf{S}}{\partial \boldsymbol{\kappa}^{\mathrm{i}}}, \quad \mathbf{H} = \frac{\partial \mathbf{C}}{\partial \mathbf{c}}. \tag{41}$$

Next, eqn (40) can be substituted into eqn (39), and the principle of virtual work (35) can be applied in order to eliminate the terms involving the variations of kinematic fields of primary and adjoint plates. Thus, after some transformations, eqn (39) finally yields

$$\delta G = \left\{ \int \{(\Psi_{,p} + w^{\mathrm{a}})\bar{\delta}p + [\Psi_{,\mathbf{M}^{\mathrm{i}}} - (\boldsymbol{\kappa}^{\mathrm{a}} - \boldsymbol{\kappa}^{\mathrm{ai}}) \cdot \mathbf{L}] \cdot \bar{\delta}\mathbf{M}^{\mathrm{i}} \right.$$

$$\left. + [\Psi_{,\kappa^{\mathrm{i}}} - (\boldsymbol{\kappa}^{\mathrm{a}} - \boldsymbol{\kappa}^{\mathrm{ai}}) \cdot \mathbf{Z}] \cdot \bar{\delta}\boldsymbol{\kappa}^{\mathrm{i}}\} \,\mathrm{d}A + \int (h_{,R_\xi} + w^{\mathrm{a}})(\delta R_\xi - R_{\xi,s}\delta\varphi_s)\,\mathrm{d}S_R \right.$$

$$+ \int (h_{,w_\xi} - R_\xi^{\mathrm{a}})(\delta w_\xi - w_{\xi,s}\delta\varphi_s)\,\mathrm{d}S_w + \int \{-[\![\Psi]\!] + [\![\mathbf{M} \cdot \boldsymbol{\kappa}^{\mathrm{a}}]\!] - [\![pw^{\mathrm{a}}]\!]$$

$$+(\mathbf{R}\cdot\mathbf{v}^{a}-\Phi)K-R_{\zeta}^{a}v_{\zeta,n}^{a}-R_{\zeta}^{a}v_{\zeta,n}+(M_{nn}v_{,s}^{a})_{,s}+(M_{nn}^{a}v_{,s})_{,s}\}\delta\varphi_{n}\,\mathrm{d}\Gamma$$

$$-\sum_{\kappa}[(h+R_{\zeta}w_{\zeta}^{a}-M_{ns}w_{,s}^{a}-M_{ns}^{a}w_{,s})\delta\varphi_{s}]\big|_{P_{k}^{s}}-\sum_{k}[(\Phi-R_{\zeta}v_{\zeta}^{a}+M_{ns}v_{,s}^{a}$$

$$+M_{ns}^{a}v_{,s})\delta\varphi_{s}-(M_{nn}v_{,s}^{a}-M_{ns}v_{,n}^{a}+M_{nn}^{a}v_{,s}-M_{ns}^{a}v_{,n})\delta\varphi_{n}]\big|_{P_{k}^{\Gamma}}$$

$$+\int[\Phi_{,c_{j}}-(v_{\zeta}^{a}-v_{\zeta}^{au})H_{\zeta j}](\bar{\delta}c_{j}+\delta_{n}c_{j})\,\mathrm{d}\Gamma\Big\}+\int\{(\psi_{,\mathbf{M}}-\boldsymbol{\kappa}^{au})\cdot\bar{\delta}\mathbf{M}$$

$$+(\Psi_{,u}-p^{a})\bar{\delta}_{n}\}\,\mathrm{d}A+\int(h_{,R_{\zeta}}+w_{\zeta}^{a})(\delta R_{\zeta}-R_{\zeta,s}\delta\varphi_{s})\,\mathrm{d}S_{w}$$

$$+\int(h_{,w_{\zeta}}-R_{\zeta}^{a})(\delta w_{\zeta}-w_{\zeta,s}\delta\varphi_{s})\,\mathrm{d}S_{R}+\int[(\Phi_{,R_{\zeta}}-v_{\zeta}^{au})(\delta R_{\zeta}-R_{\zeta,s}\delta\varphi_{s})$$

$$+(\Phi_{,v_{\zeta}}-R_{\zeta}^{au})(\delta v_{\zeta}-v_{\zeta,s}\delta\varphi_{s})]\,\mathrm{d}\Gamma. \tag{42}$$

The last four integrals on the right-hand side of eqn (42) vanish when the boundary conditions and imposed initial fields within the adjoint plate are specified as follows:

$$\tilde{w}_{\zeta}^{a}=-h_{,R_{\zeta}}\quad\text{on } S_{w},\qquad \tilde{R}_{\zeta}^{a}=h_{,w_{\zeta}}\quad\text{on } S_{R}$$

$$\kappa_{\eta\eta}^{au}=\Psi_{,M_{\eta\eta}},\qquad M_{\eta\eta}^{au}=\Psi_{,\kappa_{\eta\eta}},\qquad p^{a}=\Psi_{,w}\quad\text{within } A$$

$$v_{\zeta}^{au}=\Phi_{,R_{\zeta}},\qquad R_{\zeta}^{au}=\Phi_{,v_{\zeta}}\quad\text{along }\Gamma. \tag{43}$$

Thus, in view of conditions (43), the first variation of an arbitrary functional G is expressed by the terms in square brackets of eqn (42) and depends explicitly on shape and material variations of discontinuity line Γ, integrands of functional G and their derivatives as well as on solutions of primary and adjoint plates.

3.2. *Sensitivity analysis for complementary and potential energies*

Consider now a particular form of functional G, when it coincides with complementary or potential energy of a plate. Assume, for simplicity, the homogeneous static boundary conditions along external boundary S_R. Moreover, let there be no singular points P_k along boundaries s and Γ. The plate complementary energy is expressed in this case as

$$\Pi_{M}=\int W^{A}(\mathbf{M},\mathbf{M}^{1},\boldsymbol{\kappa}^{1})\,\mathrm{d}A+\int W^{\Gamma}(\mathbf{R},\mathbf{c})\,\mathrm{d}\Gamma-\int R_{\zeta}\tilde{w}_{\zeta}\,\mathrm{d}S_{w}. \tag{44}$$

Since, by comparing (37) with (44), we have

$$\Psi=W^{A}\quad\text{within } A,\qquad h=\begin{cases}0 & \text{on } S_{R}\\ -R_{\zeta}\tilde{w}_{\zeta} & \text{on } S_{w}\end{cases},\qquad \Phi=W^{\Gamma}\quad\text{along }\Gamma, \tag{45}$$

then, according to (43), the following conditions have to be imposed on the adjoint plate

$$\tilde{\mathbf{w}}^{a}=\tilde{\mathbf{w}}\quad\text{on } S_{w},\qquad \tilde{\mathbf{R}}^{a}=0\quad\text{on } S_{R}$$

$$\boldsymbol{\kappa}^{au}=W_{,\mathbf{M}}^{A}=\boldsymbol{\kappa},\qquad \mathbf{M}^{au}=0,\qquad p^{a}=0\quad\text{within } A$$

$$\mathbf{v}^{au}=W_{,\mathbf{R}}^{\Gamma}=\mathbf{v},\qquad \mathbf{R}^{au}=0\quad\text{along }\Gamma. \tag{46}$$

Due to conditions (46), the solutions of adjoint plate can be expressed in terms of primary fields and they take the form

$$\mathbf{w}^a = \mathbf{w}, \quad \boldsymbol{\kappa}^a = \boldsymbol{\kappa}, \quad \mathbf{M}^a = 0 \quad \text{within } A$$
$$\mathbf{v}^a = \mathbf{v}, \quad \mathbf{R}^a = 0 \quad \text{along } \Gamma. \tag{47}$$

Substituting (45)–(47) into eqn (42), the first variation of Π_M can be written as

$$\delta\Pi_M = \int (w\bar{\delta}p + W^A_{,\mathbf{M}^i} \cdot \bar{\delta}\mathbf{M}^i + W^A_{,\boldsymbol{\kappa}^i} \cdot \bar{\delta}\boldsymbol{\kappa}^i)\, dA - \int R_\zeta(\delta w_\zeta - w_{\zeta,s}\delta\varphi_s)\, dS_w$$
$$+ \int \{-[\![W^a]\!] + [\![\mathbf{M}\cdot\boldsymbol{\kappa}]\!] - [\![pw]\!] + (\mathbf{R}\cdot\mathbf{v} - W^\Gamma)K - R_\zeta v_{\zeta,n}$$
$$+ (M_{nn}v_s)_{,s}\}\delta\varphi_n\, d\Gamma + \int W^\Gamma_{,c_j}(\bar{\delta}c_j + \delta_n c_j)\, d\Gamma. \tag{48}$$

On the other hand, the plate potential energy is given in the form

$$\Pi_w = \int [U^A(\boldsymbol{\kappa}, \mathbf{M}^i, \boldsymbol{\kappa}^i) - pw]\, dA + \int U^\Gamma(\mathbf{v}, \mathbf{c})\, d\Gamma. \tag{49}$$

Comparing now (33) with (49), there is

$$\Psi = U^A - pw \quad \text{within } A, \quad h = 0 \quad \text{on } S, \quad \Phi = U^\Gamma \quad \text{along } \Gamma \tag{50}$$

and conditions (43) yield

$$\tilde{\mathbf{w}}^a = 0 \quad \text{on } S_w, \quad \tilde{\mathbf{R}}^a = 0 \quad \text{on } S_R$$
$$\boldsymbol{\kappa}^{ai} = 0, \quad \mathbf{M}^{ai} = U^a_{,\boldsymbol{\kappa}} = \mathbf{M}, \quad p^a = -\mathbf{p} \quad \text{within } A$$
$$\mathbf{v}^{ai} = 0, \quad \mathbf{R}^{ai} = U^\Gamma_{,\mathbf{v}} = \mathbf{R} \quad \text{along } \Gamma. \tag{51}$$

Thus, the solutions for the adjoint plate now have the form

$$\mathbf{w}^a = 0, \quad \boldsymbol{\kappa}^a = 0, \quad \mathbf{M}^a = -\mathbf{M} \quad \text{within } A$$
$$\mathbf{v}^a = 0, \quad \mathbf{R}^a = -\mathbf{R} \quad \text{along } \Gamma, \tag{52}$$

and the first variation of Π_w, following on from eqn (42), is expressed as

$$\delta\Pi_w \int (-w\bar{\delta}p + U^A_{,\mathbf{M}^i} \cdot \bar{\delta}\mathbf{M}^i + U^A_{,\boldsymbol{\kappa}^i} \cdot \bar{\delta}\boldsymbol{\kappa}^i)\, dA + \int R_\zeta(\delta w_\zeta - w_{\zeta,s}\delta\varphi_s)\, dS_w$$
$$+ \int \{-[\![U^A]\!] - [\![pw]\!] - U^\Gamma K + R_\zeta v_{\zeta,n} - (M_{nn}v_s)_{,s}\}\delta\varphi_n\, d\Gamma$$
$$+ \int U^\Gamma_{,c_j}(\bar{\delta}c_j + \delta_n c_j)\, d\Gamma. \tag{53}$$

Noting that $W^A + U^A = \mathbf{M}\cdot\boldsymbol{\kappa}$ and $W^\Gamma + U^\Gamma = \mathbf{R}\cdot\mathbf{v}$, we can easily verify that $\delta\Pi_M - \delta\Pi_w$.

4. OPTIMAL DESIGN OF DISCONTINUITY LINE

The typical optimal design problem involves minimization (or maximization) of any objective functional subject to the set of global or local constraints. When the global structural cost is to be minimized, the global constraints can be imposed on generalized

strains, stresses or displacements. An alternative formulation would require the minimization (or maximization) of an arbitrary functional of generalized stresses, strains or displacements, which can be expressed in the form similar to (15) or (37). In this case, the constraint can be set on the upper bound of the structural generalized cost, that is

$$\text{min. (or max.) } G \text{ subject to } \mathscr{K} - \mathscr{K}_0 = \int k(\mathbf{c})\, d\Gamma \leqslant 0 \tag{54}$$

where $k(\mathbf{c})$ denotes the specific generalized unit cost of discontinuity line Γ and $\mathscr{K}_0$ is a prescribed quantity. Introducing the Lagrange functional

$$G' = G + \lambda(\mathscr{K} - \mathscr{K}_0 + \beta^2) \tag{55}$$

where λ and β denote the Lagrange multiplier and slack variable, its stationarity condition yields the following optimality conditions:

$$\delta_c G = -\lambda \delta_c \mathscr{K}, \quad \delta_\varphi G = -\lambda \delta_\varphi \mathscr{K} \tag{56}$$

with the switching and constraint conditions of the form

$$\delta\beta = 0, \quad \delta\lambda(\mathscr{K} - \mathscr{K}_0 + \beta^2) = 0. \tag{57}$$

Here $\delta_c G$ and $\delta_\varphi G$ denote the variations of functional G with respect to variations of material parameters and the shape of the discontinuity line, whereas

$$\delta\mathscr{K} = \delta_c \mathscr{K} + \delta_\varphi \mathscr{K} = \int k_{,c_j}(\delta\bar{c}_j + \delta_n c_j)\, d\Gamma - \int k K \delta\varphi_n\, d\Gamma - \sum_i [\![k \delta\varphi_s]\!]_{P_i^1}. \tag{58}$$

The objective functional G can express, in integral form, both local and global quantities depending on generalized stresses, strains or displacements of a disk or plate. Consider, for instance, the minimization of maximal local displacement component u_i within disk domain A. The objective functional can be represented here by

$$G = \left[\int |u_i|^p\, dA \right]^{1/p}, \tag{59}$$

since for p tending to infinity, G is tending to $u_i^{\max}$. Similarly, the maximum local stress component or generalized stress intensity can be obtained by considering the functional

$$G = \left[\int \Psi^p(\mathbf{Q})\, dA \right]^{1/p} \tag{60}$$

where p is even and Ψ is assumed to be a homogeneous function of generalized stresses of the first order. In fact, for $p \to \infty$, $G \to \sup. \Psi$, that is the functional tends to the maximum value of its integrand. Another method is to apply the penalty approach. Namely, introducing the acceptable stress intensity level Ψ_0, we can consider the functional

$$G = \int \left| \frac{\Psi(\mathbf{Q})}{\Psi_0} \right|^p dA. \tag{61}$$

For $p \to \infty$ the integrand $|\Psi/\psi_0|^p$ tends to zero for $\Psi/\Psi_0 < 1$ and tends to infinity for $\psi/\psi_0 > 1$. This provides a proper penalty functional which for large p takes very small values when $\psi < \psi_0$ and very large ones when $\psi > \psi_0$.

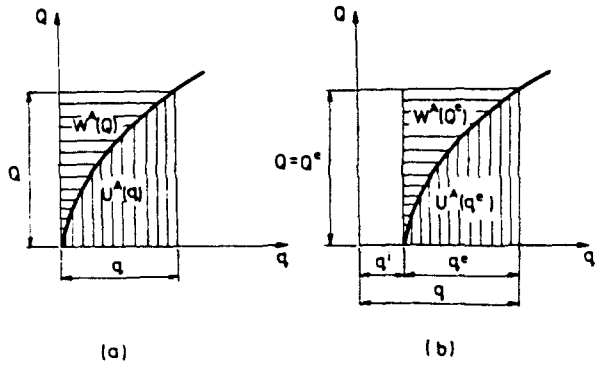

Fig. 2. Generalized stress–strain relation without initial strain (a) and with initial strain (b).

In a similar way we can convert any local quantity $\Psi(\mathbf{x}_0)$ specified at a given point $\mathbf{x}_0$ of a structure into the form (15) or (37). Using the well known property of the Dirac delta function, one can write

$$\Psi(\mathbf{x}_0) = G = \int \Psi(\mathbf{x})\delta(\mathbf{x}-\mathbf{x}_0)\,dA \tag{62}$$

and the sensitivity analysis can be performed similarly as in Section 2 or 3.

Let us now discuss the problem of mean compliance (or mean stiffness) design of a disk or plate with discontinuity line when both the external loads, initial distortions and boundary displacements are imposed on the structure. We follow here the consideration carried out by Garstecki and Mróz (1987). Consider a disk (although the foregoing analysis is also applied to a plate) and assume that the constitutive laws (1) and (5) are generated from the strain or stress energy potentials which are positive-definite homogeneous functions of the order $n/(n-1)$ and n, respectively. Thus, these equations are assumed to be of the form (cf. Fig. 2)

$$\mathbf{Q} = \mathbf{Q}^e = \mathbf{S}(\mathbf{q}-\mathbf{q}^i) = \mathbf{S}(\mathbf{q}^e) = \frac{\partial U^A(\mathbf{q}^e)}{\partial \mathbf{q}^e}$$

$$\mathbf{q}-\mathbf{q}^i = \mathbf{q}^e = \mathbf{S}^{-1}(\mathbf{Q}^e) = \frac{\partial W^A(\mathbf{Q}^e)}{\partial \mathbf{Q}^e} \quad \text{within } A$$

$$\mathbf{Q}^e \cdot \mathbf{q}^e = \frac{n}{n-1} U^A(\mathbf{q}^e) = nW^A(\mathbf{Q}^e)$$

$$\mathbf{N} = \mathbf{C}(\mathbf{v},\mathbf{c}) = \frac{\partial U^\Gamma(\mathbf{v},\mathbf{c})}{\partial \mathbf{v}}, \quad \mathbf{v} = \mathbf{C}^{-1}(\mathbf{N},\mathbf{c}) = \frac{\partial W^\Gamma(\mathbf{N},\mathbf{c})}{\partial \mathbf{N}} \quad \text{along } \Gamma$$

$$\mathbf{N} \cdot \mathbf{v} = \frac{n}{n-1} U^\Gamma(\mathbf{v},\mathbf{c}) = nW^\Gamma(\mathbf{n},\mathbf{c}) \tag{63}$$

where $\mathbf{Q} = \mathbf{Q}^e$ are the statically admissible elastic stresses, while $\mathbf{q}^e = \mathbf{q}-\mathbf{q}^i$ denote the elastic part of total strains $\mathbf{q}$, and $U^A(\mathbf{q}^e)$ and $W^A(\mathbf{Q}^e)$ are called the specific elastic strain and stress energies, respectively.

The measure of mean structure compliance, considered as a work of external load due to induced displacements, can be expressed as

$$C = \int \mathbf{N}\cdot\mathbf{u}\,dS + \int \mathbf{f}\cdot\mathbf{u}\,dA. \tag{64}$$

Assume first that there are no distortions within disk domain A and the disk is rigidly supported on boundary portion S_u. Thus the work of external forces is expressed by

$$C = \int \tilde{\mathbf{N}}\cdot\mathbf{u}\,dS_T + \int \mathbf{f}\cdot\mathbf{u}\,dA. \tag{65}$$

The potential and complementary energies are

$$\Pi_u = \int (U^A - \mathbf{f}\cdot\mathbf{u})\,dA + \int U^\Gamma\,d\Gamma - \int \tilde{\mathbf{N}}\cdot\mathbf{u}\,dS_T, \quad \Pi_Q = \int W^A\,dA + \int W^\Gamma\,d\Gamma. \tag{66}$$

By using the reciprocal theorem and eqns (63), it follows from eqns (66) that

$$\Pi_u = -\frac{1}{n-1}\left[\int U^A\,dA + \int U^\Gamma\,d\Gamma\right] = -\frac{1}{n}C, \quad \Pi_Q = \int W^A\,dA + \int W^\Gamma\,d\Gamma = \frac{1}{n}C. \tag{67}$$

Thus, both the potential and complementary energies are proportional to C and they can be regarded as measures of mean structural compliance. Equations (65) and (67) yield then the following equivalent formulations of optimal design:

$$\text{min. } C = \text{min. } \Pi_Q = \text{max. } \Pi_u = \text{min.}\left\{\int W^A\,dA + \int W^\Gamma\,d\Gamma\right\}$$
$$= \text{min.}\left\{\int U^A\,dA + \int U^\Gamma\,d\Gamma\right\}. \tag{68}$$

Consider next the case when the external load vanishes and the disk is only subjected to nonvanishing distortions and boundary displacements. Thus, the mean structural compliance is now expressed by

$$C = \int \mathbf{N}\cdot\tilde{\mathbf{u}}\,dS_u \tag{69}$$

while the potential and complementary energies equal

$$\Pi_u = \int U^A\,dA + \int U^\Gamma\,d\Gamma, \quad \Pi_Q = \int (W^A + \mathbf{Q}^e\cdot\mathbf{q}^i)\,dA + \int W^\Gamma\,d\Gamma - \int \mathbf{N}\cdot\tilde{\mathbf{u}}\,dS_u. \tag{70}$$

In view of eqns (63), these expressions can be transformed as follows:

$$\Pi_u = \int U^A\,dA + \int U^\Gamma\,d\Gamma = \frac{n-1}{n}C$$
$$\Pi_Q = -(n-1)\left[\int W^A\,dA + \int W^\Gamma\,d\Gamma\right] = -\frac{n-1}{n}C, \tag{71}$$

and once again they are proportional to C. The following equivalence of various optimal design formulations now occurs:

$$\min.\ C = \max.\ \Pi_Q = \min.\ \Pi_u = \min.\left\{\int W^A\,\mathrm{d}A + \int W^\Gamma\,\mathrm{d}\Gamma\right\}$$

$$= \min.\left\{\int U^A\,\mathrm{d}A + \int U^\Gamma\,\mathrm{d}\Gamma\right\}. \quad (72)$$

Comparing (68) with (72), it is seen that when the complementary or potential energies are to be assumed as the measure of mean compliance of structure, there is a conflicting situation in which both external loads and distortions and boundary displacements are imposed simultaneously on the structure. In fact, when, for instance, the total complementary energy is to be minimized, the structure attains minimal compliance for the case of applied load and maximal compliance for the case of imposed distortions and support displacements. Thus, for the case of simultaneous action of both loads and distortion and/or support displacements, the potential and complementary energies are not proper measures of structure behaviour. Instead of these, the total elastic strain or stress energies could be used as such measures, although there are no direct relations of these energies to the potential and complementary energies.

Following Garstecki and Mróz (1987), we can apply formally the concept of multi-objective vector optimization and use the compromise formulation by introducing the objective functional in one of the following forms:

$$G_1 = -\alpha\Pi_u^{\mathrm{l}} = \beta\Pi_u^{\mathrm{d}} = \alpha\Pi_Q^{\mathrm{l}} - \beta\Pi_Q^{\mathrm{d}} \quad (73)$$

or

$$G_2 = \alpha\mathcal{W}^{\mathrm{l}} + \beta\mathcal{W}^{\mathrm{d}} = \alpha\mathcal{U}^{\mathrm{l}} + \beta\mathcal{U}^{\mathrm{d}} \quad (74)$$

where the total elastic stress and strain energies are

$$\mathcal{W} = \int W^A\,\mathrm{d}A + \int W^\Gamma\,\mathrm{d}\Gamma, \quad \mathcal{U} = \int U^A\,\mathrm{d}A + \int U^\Gamma\,\mathrm{d}\Gamma \quad (75)$$

and $\alpha \geqslant 0$, $\beta \geqslant 0$, $\alpha+\beta = 1$. Superscripts l and d denote the energy portions calculated separately for the case of applied loads and distortions and/or support displacements. For nonlinear elastic structures, the mechanical interpretation of G_1 and G_2 is not clear. However, for linear constitutive relations and $\alpha = \beta = 1/2$ the functionals G_1 and G_2 are equal and proportional to the total elastic energy of structure. Moreover, for physically and geometrically linear structures, the total stresses $\mathbf{Q} = \mathbf{Q}^{\mathrm{e}}$ and strains $\mathbf{q}^{\mathrm{e}}$ can be regarded as superpositions of stresses $\mathbf{Q}^{\mathrm{el}}$ and strains $\mathbf{q}^{\mathrm{el}}$ due to applied loads, with vanishing distortions and support displacements, and stresses $\mathbf{Q}^{\mathrm{ed}}$ and strains $\mathbf{q}^{\mathrm{ed}}$ as corresponding to imposed distortions and displacements, with vanishing loads. In the same way, the total-elastic energies can be decomposed, namely

$$\mathcal{W}(\mathbf{Q}^{\mathrm{e}}) = \mathcal{W}(\mathbf{Q}^{\mathrm{el}}) + \mathcal{W}(\mathbf{Q}^{\mathrm{ed}}), \quad \mathcal{U}(\mathbf{q}^{\mathrm{e}}) = \mathcal{U}(\mathbf{q}^{\mathrm{el}}) + \mathcal{U}(\mathbf{q}^{\mathrm{ed}}). \quad (76)$$

Furthermore, it can be observed easily that the total elastic strain and stress energies can be regarded as the sum of partial potential or complementary energies, namely

$$\mathcal{U}(\mathbf{q}^{\mathrm{e}}) = \Pi_u^{\mathrm{d}}(\mathbf{q}^{\mathrm{ed}}) - \Pi_u^{\mathrm{l}}(\mathbf{q}^{\mathrm{el}}), \quad \mathcal{W}(\mathbf{Q}^{\mathrm{e}}) = \Pi_Q^{\mathrm{l}}(\mathbf{Q}^{\mathrm{el}}) - \Pi_Q^{\mathrm{d}}(\mathbf{Q}^{\mathrm{ed}}). \quad (77)$$

These properties provide good compromise measures of structural behaviour in the case of conflicting design objectives, namely the total elastic strain or stress energies $\mathcal{U}(\mathbf{q}^{\mathrm{e}})$ or $\mathcal{W}(\mathbf{Q}^{\mathrm{e}})$ specified by eqns (75) and satisfying the additivity conditions (76). Moreover, these energies are not sensitive to the sign or direction of distortion and load vectors.

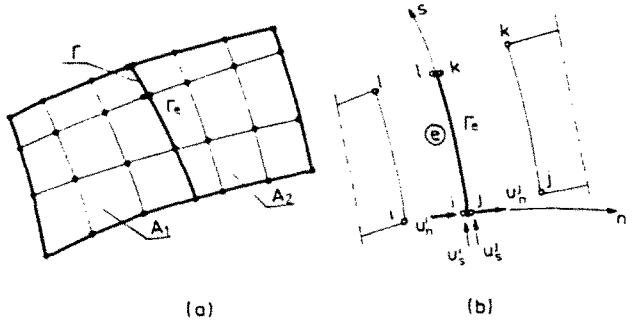

Fig. 3. Discretization of plate (a) and linking element (b).

5. NUMERICAL IMPLEMENTATION OF SENSITIVITY ANALYSIS AND OPTIMAL DESIGN

As it was shown in previous sections, the sensitivity information on any functional can be obtained as the result of solutions of primary and adjoint problems. Both analysis can be performed by using the analytical or numerical methods. When, due to complexity of the problem at hand, the numerical method of solution should be used, the most common possibility is to use the finite element method or boundary element method. Since the detailed study of various numerical approximation schemes is beyond the scope of this paper, let us discuss only some aspects of numerical implementation of sensitivity analysis through the finite element method.

The approximate finite element model of a disk or plate should ensure the possibility of a jump in generalized displacements along discontinuity line Γ, retaining simultaneously the continuity of internal tractions. Thus, when the disk or plate domain can be approximated by any kind of finite disk or plate elements, the special attention should be paid to modelling of discontinuity line through one-dimensional linking elements, for which the constitutive law is expressed by eqn (5) or (34).

Let us now discuss the derivation of a stiffness matrix of such linking elements for the case of disk subjected to stretching. The similar analysis can also be easily performed for a plate subjected to flexure. Assume that both disk domains A_1 and A_2 are approximated by a set of three- or four-node finite elements. Along a discontinuity line Γ the set of one-dimensional linking elements is introduced (cf. Fig. 3a), which carries into effect the discontinuity of generalized displacements across Γ, retaining the continuity of internal tractions. Each linking element has two nodal points at each end (cf. Fig. 3b), and the nodal displacements and forces of element e are denoted by $\{\Delta^e\}$ and $\{F^e\}$. The displacements on the right- and left-side of boundary Γ^e and their jump can be expressed in the form

$$\{u^r\} = [\mathcal{N}^r]\{\Delta^e\}, \quad \{u^l\} = [\mathcal{N}^l]\{\Delta^e\}$$
$$\{v^e\} = \{u^r\} - \{u^l\} = ([\mathcal{N}^r] - [\mathcal{N}^l])\{\Delta^e\} = [\mathcal{N}]\{\Delta^e\} \tag{78}$$

where $[\mathcal{N}^{r,l}]$ denotes the common set of element unit functions. Let now the constitutive law (5), relating internal forces $\{N^e\}$ to the jump of displacements $\{v^e\}$, be assumed in the form

$$\{N^e\} = [C(\{v^e\}, \mathbf{c})]\{v^e\}. \tag{79}$$

The virtual work done by internal forces $\{N^e\}$ and nodal forces $\{F^e\}$ are equal:

$$\int \{\delta v^e\}^T \{N^e\}\, d\Gamma^e = \{\delta\Delta^e\}^T \int [\mathcal{N}]^T [C][\mathcal{N}]\, d\Gamma^e \{\Delta^e\}, \quad \{\delta\Delta^e\}^T\{F^e\}. \tag{80}$$

Comparing the work of both these, the following equation can be obtained:

$$[k^e]\{\Delta^e\} = \{F^e\} \tag{81}$$

where the stiffness matrix of a linking element e has the form

$$[k^e] = \int [\cdot\,\Psi^{\cdot}]^T [C(\{t^e\}, \mathbf{c})][\cdot\,\Psi^{\cdot}]\, d\Gamma^e. \tag{82}$$

Assembling the stiffness matrices of all disk and linking elements, the total stiffness matrix $[K]$ can be obtained and the analysis of the disk can be performed. The solution of the primary problem is then described by a matrix equation:

$$[K(\{\Delta\})]\{\Delta\} = \{F\} \tag{83}$$

where $\{\Delta\}$ denotes a vector of nodal generalized displacements and $\{F\}$ is a vector of nodal generalized forces due to external load. When the problem is linear, eqn (83) can be solved in one step, while for physical nonlinearity the iterative algorithm should be used. Knowing the solution of the primary structure, the nodal forces $\{F^a\}$ of the adjoint structure due to applied adjoint load and the adjoint initial strains and/or stresses and body forces can be calculated and next the adjoint linear structure can be solved by using the matrix equation

$$[K^a]\{\Delta^a\} = \{F^a\}. \tag{84}$$

We should note that the adjoint stiffness matrix $[K^a]$ and primary stiffness matrix $[K]$ at the solution point are the same, in which case the cost of the adjoint solution is considerably reduced. Using the nodal values of primary and adjoint displacements the strain and stress fields of both primary and adjoint structures can be easily calculated in post-processing procedure, and the numerical approximation of sensitivity expressions (20) or (42) can be evaluated. Since these expressions depend mainly on stresses and strains evaluated along the discontinuity line, their numerical approximation requires us to calculate the stress distribution along element boundaries adjacent to Γ. In order to improve the accuracy of calculated boundary stresses the Loubignac's iterative algorithm (cf. Cook, 1982), can be, for instance, incorporated into the solution algorithm for both primary and adjoint structures.

6. SENSITIVITY ANALYSIS FOR BEAM WITH DISCONTINUITY POINT

The results obtained in Section 3 for a plate with hinge or slip line can be very easily particularized for the case of a beam. Consider then a beam of length l with a hinge or slip point at $x = s$ within its domain, and denote beam deflection, curvature and bending moment by w, κ and M, respectively. The beam generalized forces $\mathbf{R}$ are the shear force Q and bending moment M. Let the beam be loaded by external lateral pressure p and concentrated forces $\tilde{\mathbf{R}}$ at some specified points and subjected to imposed fields of initial curvature κ^i and bending moment M^i. The generalized displacements $\tilde{\mathbf{w}}$ are prescribed at fixed points where the beam is supported. The stress–strain relations within the beam domain and at the discontinuity point are assumed to be of the forms (33) and (34), respectively.

As for the case of plate, we consider the first variation with respect to the variation of discontinuity point location of the following functional:

$$G = \int_0^l \Psi(M, \kappa, p, w, M^i, \kappa^i)\, dx + h(R_\xi, w_\xi) + \Phi(R_\xi, v_\xi, \mathbf{c}) \tag{85}$$

where function h can be specified at all points with prescribed $\tilde{\mathbf{R}}$ and $\tilde{\mathbf{w}}$, and Φ is specified at the hinge/slip point. The first variation of functional (85) follows from (42), and then it is expressed by

$$\delta G = \int_0^l \{(\Psi_{,p} + w^{\mathrm{a}})\bar{\delta}p + [\Psi_{,M^{\mathrm{a}}} - (\kappa^{\mathrm{a}} - \kappa^{\mathrm{a}\mathrm{i}})L]\bar{\delta}M^{\mathrm{a}} + [\Psi_{,\kappa} - (\kappa^{\mathrm{a}} - \kappa^{\mathrm{a}\mathrm{i}})Z]\bar{\delta}\kappa^{\mathrm{a}}\}\,\mathrm{d}x$$

$$+ \{-[\![\Psi]\!] + [\![M\kappa^{\mathrm{a}}]\!] - [\![pw^{\mathrm{a}}]\!] - R_\zeta^{\mathrm{a}} v_{\zeta,n}^{\mathrm{a}} - R_\zeta^{\mathrm{a}} v_{\zeta,ns}^{\mathrm{a}}\}|_{x=s}\delta s + [\Phi_{,c_j} - (v_\zeta^{\mathrm{a}} - v_\zeta^{\mathrm{a}\mathrm{i}})H_{\zeta j}](\bar{\delta}c_j + \delta_s c_j) \quad (86)$$

where $\delta_s c_j$ denotes the variation of material parameters of hinge or slip point due to variation of its position. The adjoint state fields are obtained here as the solution of adjoint beam with the following boundary conditions and imposed initial fields (cf. (43)):

$$\tilde{w}_\zeta^{\mathrm{a}} = -h_{,R_\zeta}, \quad \tilde{R}_\zeta^{\mathrm{a}} = h_{,w_\zeta}, \quad \kappa^{\mathrm{a}\mathrm{i}} = \Psi_{,M}, \quad M^{\mathrm{a}\mathrm{i}} = \Psi_{,\kappa},$$

$$p^{\mathrm{a}} = \Psi_{,w} \quad \text{for } 0 \leqslant x \leqslant l, \quad v^{\mathrm{a}\mathrm{i}} = \Phi_{,R_\zeta}, \quad R^{\mathrm{a}\mathrm{i}} = \Phi_{,v_\zeta} \quad \text{at } x = s, \quad (87)$$

whereas the stress–strain relations are of the form similar to (36).

For the particular forms of functional G coinciding with beam complementary or potential energies, the sensitivity expression (86) can be expressed in terms of primary solutions only, similarly to the way it was shown in Section 3.2 for the case of plate.

7. ILLUSTRATIVE EXAMPLES

To illustrate the analysis presented in previous sections let us consider some simple disk, beam and plate examples in which the sensitivity analysis with respect to shape of discontinuity line or location of discontinuity points for some global functionals will be performed using the analytical and numerical methods of analysis.

Example 1

Consider a circular disk of external radius r_{e} with a central hole of radius r_{i} composed of two different linear elastic materials with elastic constants E_{e}, ν_{e} and E_{i}, ν_{i}, respectively. These materials are separated by a dilatancy line of radius R and constant stiffness c (Fig. 4). The disk is rigidly supported along outer edge and loaded by the uniform pressure p_{i} along hole edge. Furthermore, the disk is subjected to the imposed field of initial strains caused by temperature field T. The inner and outer temperatures T_{i} and T_{e} are prescribed on both disk edges. The thermal conductivities and coefficients of thermal expansion of both materials are denoted by λ_{e}, α_{e} and λ_{i}, α_{i}, respectively. Due to geometrical and mechanical symmetry, the nonvanishing stress components within both disk domains are radial and circumferential generalized stresses $N_{r\mathrm{e}}$, $N_{\vartheta\mathrm{e}}$ and $N_{r\mathrm{i}}$, $N_{\vartheta\mathrm{i}}$, while the radial displacements are denoted by u_{e} and u_{i}. The interface traction N_r along the dilatancy line is proportional to the jump of radial displacements and can be written as

$$N_r(R) = cv(R) = c[u_{\mathrm{e}}(R) - u_{\mathrm{i}}(R)]. \quad (88)$$

The optimization problem can now be formulated as follows: for various combinations of inner pressure and initial strains caused by prescribed boundary temperatures find the optimal locations of the dilatancy line, which minimize the total elastic stress energy of the disk. As it was shown in Section 4, this energy provides a good compromise measure of

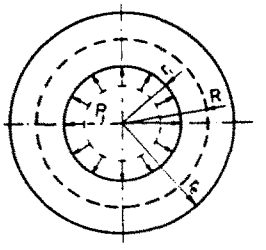

Fig. 4. Circular disk with dilatancy line.

structural behaviour in the case of conflicting interaction of external load and initial distortions. In view of (75), the total elastic stress energy is now expressed as

$$\mathscr{W} = \frac{1}{2E_i}\int_{r_i}^{R}[(N_{ri}+N_{si})^2-2(1+\nu_i)N_{ri}N_{si}]r\,\mathrm{d}r+\frac{1}{2E_e}\int_{R}^{r_e}[(N_{re}+N_{se})^2$$

$$-2(1+\nu_e)N_{re}N_{se}]r\,\mathrm{d}r+\frac{1}{2c}N_r^2R\to\min_R. \quad (89)$$

The optimality condition follows from (56) and in view of (20) and (89) it can be written in the form

$$\delta\mathscr{W} = \int_{r_i}^{r_e}\alpha(N_r+N_s)\delta T r\,\mathrm{d}r-\left\{[\![W^A]\!]-([\![N_s u^a]\!]-N_r[\![u^a]\!]+W^\Gamma)\frac{1}{R}+N_r^a[\![u_r]\!]\right\}R\delta R=0 \quad (90)$$

where δT denotes the variation of temperature field within disk domain. The adjoint disk satisfies now the homogeneous boundary conditions on both edges and is subjected to the imposed field of initial strains, which are

$$\varepsilon_r^{ai}=\frac{1}{E}(N_r-\nu N_s)=\varepsilon_r^e,\quad \varepsilon_s^{ai}=\frac{1}{E}(N_s-\nu N_r)=\varepsilon_r^e \quad (91)$$

where ε_r^e and ε_s^e are the elastic part of total strains ε_r and ε_s of primary disk. Furthermore, along the dilatancy line the initial jump of radial displacements is introduced, namely

$$v^{ai}(R)=\frac{NR}{c}=v(R). \quad (92)$$

Solving the primary and adjoint problems, the value of functional $\mathscr{W}$ and its derivative $\delta\mathscr{W}/\delta R$ were calculated for various locations of dilatancy line. Figure 5 shows the results of calculations for two particular cases of loading conditions for a disk of radii $r_i = 0.2$ m and $r_e = 1.0$ m. It was assumed that the disk was made of steel and aluminium with the following material data: $E_i = 2.1\times10^5$ MPa, $\nu_i = 0.29$, $\alpha_i = 1.6\times10^{-5}\,°C^{-1}$, $\lambda_i = 3.6$ cal $ms^{-1}\,°C^{-1}$ and $E_e = 0.7\times10^5$ MPa, $\nu_e = 0.33$, $\alpha_e = 2.3\times10^{-5}\,°C^{-1}$, $\lambda_e = 55$ cal $ms^{-1}\,°C^{-1}$. The stiffness of dilatancy line was assumed to be $c = 1.4\times10^6$ MPa m^{-1}. The outer edge of disk was rigidly supported and kept in the temperature $T_e = 0°C$.

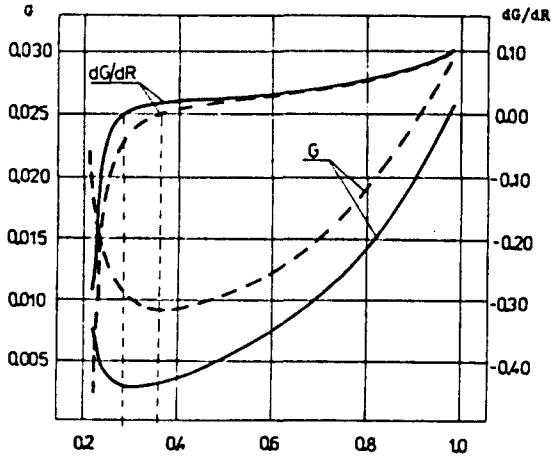

Fig. 5. Total elastic stress energy of disk and its derivative versus location of dilatancy line.

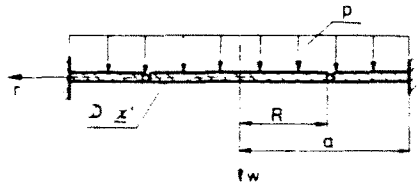

Fig. 6. Circular plate with hinge line.

The plots of total elastic stress energy (89) and its derivative calculated by using eqn (90) for various radii R of dilatancy line, for the case of vanishing internal pressure p_i and prescribed internal temperature $T_i = -100$ C, are shown with the solid line in Fig. 5. It is seen that the functional $\mathscr{U}^*$ attains its global minimum for the optimal value of $R = 0.302$ m. The case when the inner edge of disk is subjected to the temperature $T_i = -100$ C and pressure $p_i = 2000$ MPa is shown with the dashed line. For this case of loading the optimal value of radius of dilatancy line is equal to 0.367 m.

Example II

Consider now a circular plate of external radius a with hinge line of radius R (Fig. 6). The plate is made of linear plastic material and its bending rigidity is denoted by D, while the hinge line has a constant stiffness c. The outer edge of plate is rigidly supported and the uniform lateral pressure p, as well as an imposed field of constant initial distortion $\kappa_r^1 = \kappa_\vartheta^1 = \kappa^1$, is applied to the plate. These initial distortions can be caused, for instance, by a difference in temperature between lower and upper plate surfaces. The nonvanishing stress components within both plate domains are denoted by M_{ri}, $M_{\vartheta i}$ and M_{re}, $M_{\vartheta e}$, while the deflections are w_i and w_e. The shear force Q is continuous along the hinge line and the normal moment M_r transformed through this line is proportional to the jump of normal derivatives of deflection fields, namely

$$M_r = M_{ri}(R) = M_{re}(R) = c(w_{i,r} - w_{e,r}). \tag{93}$$

We can now formulate the following optimization problem: for various combinations of lateral pressure p and initial curvature κ^1 find the optimal radius of the hinge line, which minimizes the maximum effective moment within plate domain:

$$\min_{0<R<a} \left\{ \max. M_e(x) = \sqrt{M_r^2 + M_\vartheta^2 - M_r M_\vartheta} \right\}. \tag{94}$$

In view of (60), the local objective function (94) can be converted to the integral form and the problem can be stated as follows:

$$\min_{0<R<a} \bar{G} = G^{1/n} = \left\{ \int_0^a M_e^n r \, dr \right\}^{1/n} = \left\{ \int_0^a (\sqrt{M_r^2 + M_\vartheta^2 - M_r M_\vartheta})^n r \, dr \right\}^{1/n} \tag{95}$$

where n is even and tending to infinity. The optimality condition of the problem (95) follows from eqns (56) and is simplified to the form

$$\delta_R \bar{G} = \frac{1}{n} G^{(1-n)/n} \delta_R G = 0 \tag{96}$$

where $\delta_R G$ is expressed by (42). Thus, it follows from (96) and (42) that the optimality condition of the problem considered can be written in the form

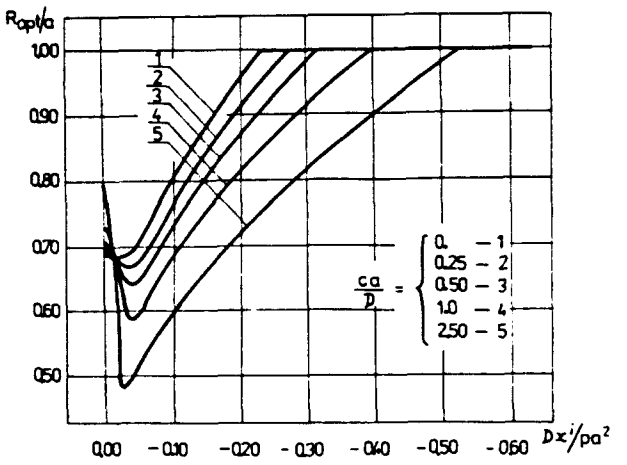

Fig. 7. Optimal location of hinge line.

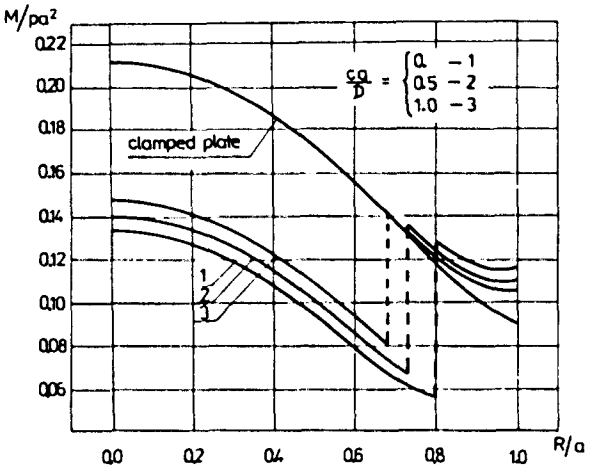

Fig. 8. Effective moment versus location of hinge line.

$$\left\{-[\![M_c^a]\!]-[\![M_s w_{,r}^a]\!]\frac{1}{R}+M_r[\![w_{,r}^a]\!]\frac{1}{R}+M_r^a[\![w_{,rr}]\!]\right\}R|_{r=R}=0. \tag{97}$$

The adjoint fields w^a, $\mathbf{M}^a$ appearing in (97), are obtained as the solution for the adjoint plate with homogeneous boundary conditions, subjected to the imposed field of initial curvature $\boldsymbol{\kappa}^i$ following on from (43), that is

$$\kappa_r^{ai} = M_{c,M_r}^n = nM_c^{n-2}(M_r - \tfrac{1}{2}M_s), \quad \kappa_s^{ai} = M_{c,M_s}^n = nM_c^{n-2}(M_s - \tfrac{1}{2}M_r). \tag{98}$$

The results of the numerical solution of optimality condition (97) are shown in Fig. 7, where the plot of the optimal radius of the hinge line versus the ratio of initial curvature to lateral pressure is given for different values of hinge stiffness. In Fig. 8 the distribution of effective moment along the radius of the plate with optimal location of hinge line is given for three different values of hinge stiffness, and $D\kappa^i/pa^2 = -0.1$. The similar plot for a clamped plate without any hinge line is also shown. It is observed that on introducing the optimal hinge line within the plate domain, the maximal effective moment in its domain is reduced by about 35% in comparison with the plate without any hinges.

Example III

As the last example, consider a beam of span l and constant rigidity D, clamped at both ends (Fig. 9), for which the sensitivities can be expressed in analytical form. A uniform load p is applied to the beam and initial distortions are imposed in the form of initial curvature κ^i within its domain and deflection w_0 at its end B. For various combinations of loading and distortion we are looking for the optimal location s of the free hinge C, which will minimize the total elastic stress energy of the beam

$$\mathscr{W} = \int_0^l W(M)\,\mathrm{d}x = \int_0^l \frac{M^2}{2D}\,\mathrm{d}x \to \min_s. \tag{99}$$

The optimality condition for the problem (99) follows from (50) and (86) and takes the form

$$\frac{\delta \mathscr{W}}{\delta s} = \{Q[\![w^a_{,x}]\!] + Q^a[\![w_{,x}]\!]\}|_{x=s} = 0 \tag{100}$$

where, according to (87), the adjoint beam is subjected to initial distortion $\kappa^{ai} = \partial W/\partial M = \kappa^c$.

Introducing the nondimensional quantities

$$K = 100\kappa^i l, \quad \Delta = 100\frac{w_0}{l}, \quad P = \frac{pl^3}{D}, \quad \xi = \frac{s}{l} \tag{101}$$

the solutions of primary and adjoint beams yield

$$Q(s) = -\frac{D}{l^2}\frac{3}{1-3\xi+3\xi^2}\left(\frac{1-2\xi}{200}K + \frac{4\xi^3-6\xi^2+4\xi-1}{8}P + \tfrac{1}{100}\Delta\right)$$

$$[\![w_{,x}(s)]\!] = \frac{1}{1-3\xi+3\xi^2}\left(\tfrac{1}{400}K - \frac{1-6\xi+6\xi^2}{48}P + \frac{3(1-2\xi)}{200}\Delta\right) \tag{102}$$

and

$$Q^a(s) = -\frac{D}{l^2}\frac{3}{1-3\xi+3\xi^2}\left(\frac{1-2\xi}{200}K + \tfrac{1}{100}\Delta\right)$$

$$[\![w^a_{,x}(s)]\!] = \frac{1-6\xi+6\xi^2}{48(1-3\xi+3\xi^2)}P. \tag{103}$$

Now using eqns (102) and (103) in eqn (100), we obtain the following equation:

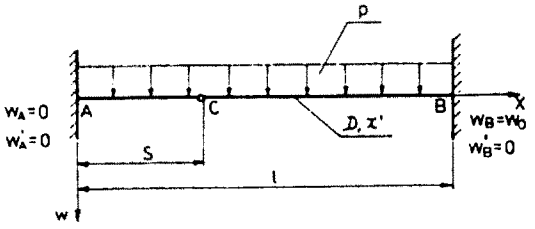

Fig. 9. Beam with hinge.

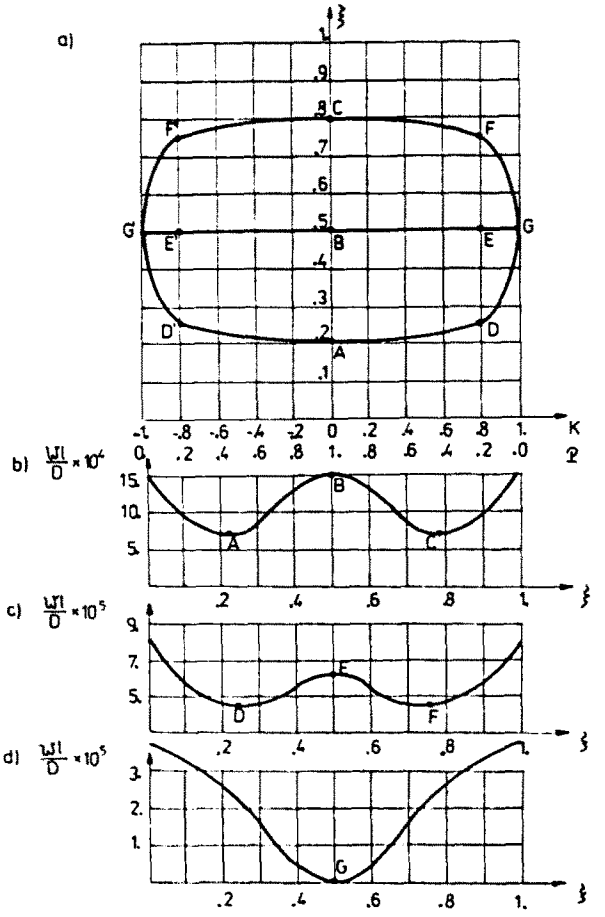

Fig. 10. Optimal hinge location for the interaction of load and initial curvature.

$$\overset{0.25}{\xi^4}(4\xi^3+6\xi^2+4\xi-1)(1-6\xi+6\xi^2)P^2+\left(\frac{1-2\xi}{2}K+\Delta\right)\left(\frac{3-6\xi}{2}\Delta-\tfrac{1}{2}K\right)=0 \quad (104)$$

from which the optimal solutions ξ_{opt} can be generated for various combinations of P, K and Δ. To present the results let us assume that Δ and K vary within the interval $\langle -1, +1\rangle$, whereas P varies within $\langle 0, 1\rangle$ and $P+|K| = 1$. This last normalization assumption guarantees that the whole range $-\infty < K/P < +\infty$ will be taken into consideration. The optimal hinge locations ξ_{opt} following from (104) are presented in Fig. 10a for $\Delta = 0$ and in Fig. 11a for $K = 0$.

When the beam is subjected to external load with vanishing initial curvature κ^i and support deflection w_0, there are two equivalent optimal solutions $\xi_{1,2} = 1/2 \pm \sqrt{3}/6$, represented by points A and C on the ξ axes in Figs 10a and 11a. They correspond to the stiffest beam, as it is shown in Figs 10b and 11b, where the total elastic stress energy versus varying hinge location is plotted. The point B in Figs 10a and 11a, for which $\xi = 1/2$, represents the local maximum of the functional (99). When now the beam is subjected to the initial curvature only, the optimal solution of (104) is represented by points G and G' in Fig. 10a, for which $\xi_{opt} = 1/2$. This design corresponds to the global maximum of total elastic stress energy, as can be observed in Fig. 10d. For the simultaneous action of external load and initial curvature, the optimal hinge location is represented by the curves G'F'CFG and G'D'ADG in Fig. 10a, which correspond to global minima of stress energy. The straight line G'E'DEG in Fig. 10a illustrates the local maxima of this energy. Figure 10c shows the plot of beam stress energy for simultaneous action of p and κ^i.

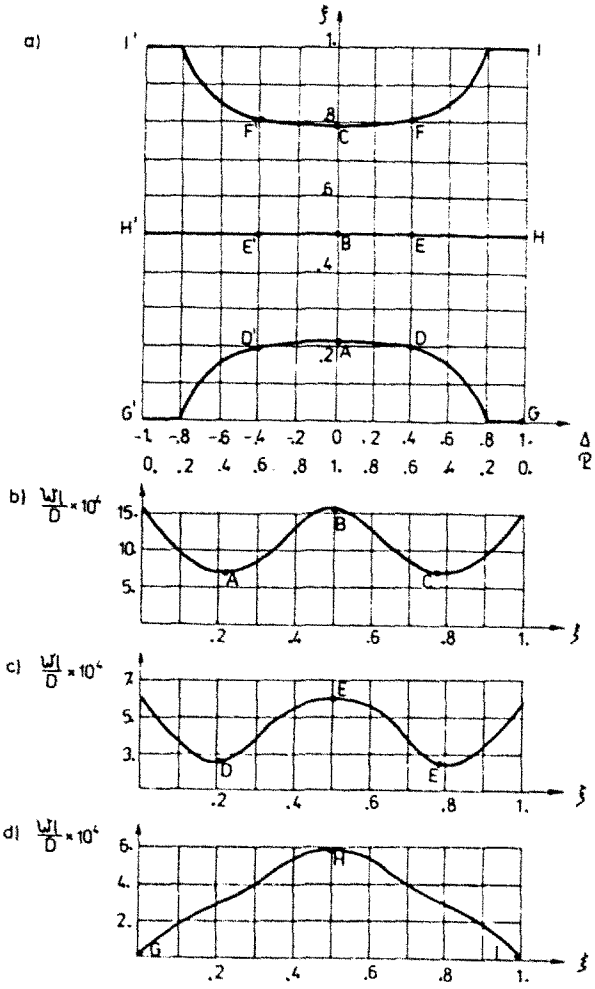

Fig. 11. Optimal hinge location for the interaction of load and support deflection.

Let us now discuss the case when the beam is subjected to external load p and support deflection w_0. The optimal location of the hinge for vanishing external load is represented by points H and H', for which $\xi_{opt} = 1/2$ and the total elastic stress energy attains its global maximum (cf. Fig. 11d). For simultaneous action of p and w_0, the optimal compromise solutions are illustrated by the curves I'F'CFI and G'D'ADG in Fig. 11a, whereas the straight line H'E'BEH corresponds to the local maxima of stress energy, as it is shown in Fig. 11c.

8. CONCLUDING REMARKS

The present analysis supplements the results of previous works, where the problems of varying external boundaries, interfaces and varying traction discontinuity lines were considered for disks and plates. In the paper, an extended class of sensitivity analysis and optimization problems is considered, for which disks, plates and beams with kinematic discontinuity lines are subjected to both external loads and distortion or boundary displacements. A general variational method to treat the problems of sensitivity analysis is discussed by considering varying dilatancy, slip or hinge lines within structure domain. The sensitivities of arbitrary differentiable functionals are expressed explicitly in terms of primary and adjoint state fields. These expressions can then be used in both analytical and numerical solutions for optimal design or identification problems.

The present paper also casts some light on the important design case where both applied loads and displacements or distortions are imposed on the structure. In such cases the compromise design should be developed, satisfying both stiffness and stress constraints.

Besides its direct application in sensitivity analysis and structural design, the formalism of this paper can be used in the theory of mechanisms with rigid or elastic links where concentrated rotations or slips occur in hinges or hinge lines. The sensitivity of both kinematic and static fields with respect to hinge location can be performed by following the present approach. The other area of application is provided by the perfect plasticity model where hinges or velocity discontinuity lines occur in any failure mechanism and the plastic dissipation occurs both within plastic zones and along the discontinuity lines. The optimal design study is then usually associated with variation of such failure mechanisms due to design modification. Such novel applications will be discussed in separate papers.

Acknowledgement—This research work was carried out within Polish Academy of Science Grant No. CPBP 02.01.

REFERENCES

Cook, R. D. (1982). Loubignac's iterative method in finite element elastostatics. *Int. J. Numer. Meth. Engng* **18**, 67–75.

Dems, K. and Mróz, Z. (1984). Variational approach by means of adjoint system to structural optimization and sensitivity analysis. *Int. J. Solids Structures* **20**(6), 527–552.

Dems, K. and Mróz, Z. (1987). Variational approach to sensitivity analysis and structural optimization of plane arches. *Mech. Struct. Mach.* **15**(3), 297–321.

Dems, K. and Mróz, Z. (1989). Sensitivity analysis and optimal design of physically nonlinear plates. *Arch. Mech.* **41**(4), 481–501.

Dems, K., Mróz, Z. and Szelag, D. (1989). Optimal design of ribstiffeners in disks and plates. *Int. J. Solids Structures* **25**(9), 973–998.

Garstecki, A. (1988). Optimal design of joints in elastic structures. *Acta Mech.* **75**, 63–76.

Garstecki, A. and Mróz, Z. (1987). Optimal design of elastic structures subjected to loads and initial distortions. *Mech. Struct. Mach.* **15**(1), 47–68.

Mróz, Z. (1986). Variational approach to shape sensitivity analysis and optimal design. In *The Optimum Shape* (Edited by J. A. Bennett and M. E. Botkin), pp. 79–111. Plenum Press, New York.

Mróz, Z. (1987). Sensitivity analysis and optimal design with account for varying shape and support conditions. *Proc. NATO ASI: Computer Aided Optimal Design: Structural and Mechanical Systems* (Edited by C. A. Mota Soares), pp. 407–439. Springer, Berlin.